

Probabilistic Load Flow for Correlated Wind Power and Storage Extension

Master Thesis

eingereicht an der Technischen Universität Wien,
Fakultät für Elektrotechnik und Informationstechnik
zum Zwecke der Erlangung des akademischen Grades
Diplom-Ingenieur

betreut von

Em.O.Univ.Prof. Dipl.-Ing. Dr.-Ing. Günther Brauner
Univ.Ass. Dipl.-Ing. Franz Zeilinger, BSc

von

Harald FRANCHETTI, BSc

Matrikelnummer: e0326154

Johann Patzelt-Gasse 3

AT-2700 Wiener Neustadt

Vienna, June 2014

Advisors:

Em.O.Univ.Prof. Dipl.-Ing. Dr.-Ing. Günther Brauner

Institute of Energy Systems and Electrical Drives, Vienna University of Technology, AT

Univ.Ass. Dipl.-Ing. Franz Zeilinger, BSc

Institute of Energy Systems and Electrical Drives, Vienna University of Technology, AT

Gabriela Hug-Glanzmann, PhD

Department of Electrical and Computer Engineering, Carnegie Mellon University, USA

Danksagung

Ich danke ganz herzlich bei meinen Eltern Traude und Franz. Sie haben mir dieses Studium ermöglicht, mich immer bestmöglich unterstützt und waren immer für mich da. Danke!

Weiters bedanke ich mich natürlich auch bei meinen beiden Brüdern Franz und Thomas, die mich immer beraten, mich bestärkt sowie ermuntert haben.

Großer Dank gebührt auch all meinen Freunden und Studienkollegen, die mir immer behilflich waren und mit Rat und Tat zur Seite standen und mit denen ich eine unvergessliche Studienzeit verbringen durfte.

Im Speziellen danke ich auch Prof. Günther Brauner und Franz Zeilinger für die gute Betreuung und Unterstützung bei dieser Arbeit.

Bei Gabriela Hug-Glanzmann möchte ich mich sehr herzlich für ihre Unterstützung und das Ermöglichen meines Auslandsaufenthaltes in den Vereinigten Staaten bedanken. Dadurch konnte ich den wissenschaftlichen Teil dieser Arbeit an der Carnegie Mellon University in Pittsburgh, PA durchführen und die damit verbundenen, sehr wertvollen Erfahrungen eines Studienaufenthaltes im Ausland sammeln

Diese Arbeit entstand somit in Kooperation zwischen dem *Department of Electrical and Computer Engineering* der Carnegie Mellon University in Pittsburgh (PA), USA und der *Arbeitsgruppe Elektrische Anlagen* am Institut für Energiesysteme und Elektrische Antriebe der Technischen Universität Wien, Österreich.

Finanziell wurde mein US-Auslandsaufenthalt durch die Marshall Plan Foundation mit dem *Marshall Plan Scholarship*-Programm sowie vom Land Niederösterreich mit einem *Top-Stipendium Ausland* unterstützt.

Großer Dank geht auch an Johannes H. Schmiedt, der mir viel Zeit durch Korrekturlesen geopfert hat.

Wiener Neustadt, Juni 2014

Harald Franchetti

Acknowledgement

The research part of this master thesis has been carried out at the Department of Electrical and Computer Engineering within the Electrical Energy Systems Group at Carnegie Mellon University in Pittsburgh (PA), USA.

This work is a result of a cooperation between the Department of Electrical and Computer Engineering and the Department of Power Systems within the Institute of Energy Systems and Electrical Drives at Vienna University of Technology, Austria.

It was financially supported by the Austrian Marshall Plan Foundation through the *Marshall Plan Scholarship*-program as well as by the Federal State of Lower Austria through a *Top-Stipendium Ausland*.

Kurzfassung

Immer öfter treten Naturkatastrophen auf, die weltweitem CO₂-Ausstoß und dem daraus resultierenden Klimawandel zugeordnet werden. Große Hoffnung wird in die *erneuerbaren Energien* gesetzt, um die Emissionen zu reduzieren; vor allem Sonnen- und Windenergie werden verstärkt forciert und ausgebaut.

Diese Diplomarbeit soll einen Beitrag leisten, um die noch vielen offenen Fragen und ungelösten Probleme rund um die volatilen, erneuerbaren Energieträger schrittweise behandeln und letztendlich auch lösen zu können.

Wir haben für unsere Simulationen die Auswirkung der Korrelation zweier Windparks und deren Lasteinspeisung betrachtet. Mit der Korrelation wird die geographische Distanz beider Standorte als Windabhängigkeit modelliert.

Die Erzeugungscharakteristik eines Windparks kann sehr gut durch eine β -Verteilung dargestellt werden. Daher stand die Erzeugung von β -verteilten Zufallsvariablen mit einer bestimmten Korrelation im Mittelpunkt.

Wir wenden das DC-Lastfluss Modell auf ein kleines Testsystem an. Dieses besteht aus zwei Windparks, einer Last mit Weibull-Verteilung und einem Slack. Die Berechnungen wurden für alle wichtigen Leitungen und zwei Szenarien durchgeführt.

Einerseits wurden zwei Parks mit gleicher Wahrscheinlichkeitsverteilung für den gesamten Bereich von keiner bis zur vollen Korrelation simuliert.

Andererseits haben wir zwei unterschiedliche Windparks betrachtet und von keiner bis zur maximal möglichen Korrelation der beiden Verteilungen untersucht. Diese hängt von der Ähnlichkeit der beiden β -Verteilungen ab.

Als weiteres Szenario wurden noch Speicher und Leitungslimits einbezogen. Die Speicher wurden bei jedem Knoten angebunden und ermöglichen eine ungekürzte Produktion bei Einführung von Limits. Es wurde keine Einschränkungen auf eine bestimmte Speichertechnologie vorgenommen.

Mit unserer Korrelationsmethode können wir Gruppen von β -verteilten Zufallszahlen mit einer exakten, vorgegebenen Korrelation erzeugen. Unsere Simulationen ergeben, dass relativ einfach die minimale und maximale Belastung der Leitung ermittelt werden kann - dazu müssen die Lastfluss-Ergebnisse für keine und maximale Korrelation überlagert werden.

Abstract

This master thesis deals with probabilistic power flow analysis for correlated, β -distributed wind power injections.

The importance of *renewable energies* steadily increases over time. Wind and solar energy are playing an ever increasingly significant role in the field of climate change and smart grid applications.

In this research we focused on wind energy. We looked specifically at the correlation between wind power injections of different wind power farms. The correlation models the geographical distance between these wind power plant sites. The output of wind power plant farms can be described best by the means of probability density functions with β -distributions. We developed an algorithm to generate a set of β -distributed random variables to fit the desired correlation as closely as possible.

Our simulation method is DC-load flow and uses power transfer distribution factors. We applied our method to a small grid with two wind power injections and one load with Weibull distribution as well as a slack. We investigated the power flow on the important branches for a range from non to maximum correlation for two scenarios with different input densities.

Firstly, we investigated the situation for two equal wind parks and calculated the line flow for the correlation range from zero to full correlation.

Secondly, we repeated the simulations with differing β -distributed power outputs for both of the wind farms. The range of correlation does not even come to full correlation. The maximum correlation level depends on the similarity of the input probability densities.

We also took certain line limits into account and used storage devices for keeping the energy surplus to avoid curtailment of energy production or overloading of lines. The storage devices are placed at each bus, but do not represent a specific technology.

With our methodology of correlation we can generate exact sets of correlated, β -distributed random variables. Our simulation method can easily find the absolute maximum and minimum load on a given line just by combining the outcome of the maximum correlation and the uncorrelated result.

Contents

1	Introduction	1
1.1	Motivation	1
1.2	Problem Statement	3
1.3	Contributions of this Thesis	6
2	Background	7
2.1	Power Flow	7
2.1.1	AC Power Flow	7
2.1.2	DC Power Flow	7
2.2	Power Transfer Distribution Factor	8
2.3	Methods for Probabilistic Power Flow	10
2.4	Power Output Characteristics of Wind Farms	13
2.5	Constitutive Probability Distributions	14
2.5.1	γ -Distribution	14
2.5.2	β -Distribution	14
2.6	Linear Correlation	15
2.7	Generation of Correlated Random Variables	16
2.7.1	Uniformly Distributed and Correlated Random Variables Transformed to Desired Distribution	16
2.7.2	Dirichlet Distribution	17
2.7.3	Shared Random Variables for Correlation	17
3	Methodology of Correlation	18
3.1	Application of Available Methods	18
3.2	Adaptation for Better Correlation	20
3.3	Summation of Two Random Variables	23
3.4	Linearity Error Compensation	28
3.5	Linear Interpolation of Two Correlated Probabilistic Density Functions	34

4 Probabilistic Power Flow for Wind	37
4.1 Monte Carlo Simulation	37
4.1.1 Model	37
4.1.2 Input and Output	39
4.1.3 Method	40
4.1.4 Scalability	41
4.2 Storage	42
4.3 Line Limits	44
5 Results & Discussion	45
5.1 Identical Wind Farms	45
5.2 Different Wind Farms	52
5.3 Line Limit and Storage Extension	58
6 Conclusion	60
List of Figures	63
List of Tables	65
List of Abbreviations	66
Bibliography	67

Chapter 1

Introduction

1.1 Motivation

Electricity plays a significant role in the progress of prosperity and technology. During the last centuries electricity has been available to the industry and private households in most countries of the world. Generation of electricity was of utmost importance to achieve technological progress. However, almost the entire electricity production was not accomplished in an environmentally compatible fashion or form. Even today, worldwide electricity consumption grows every year and the generation becomes more efficiently and environmentally friendly. In Fig. 1.1, we see both, the historical, as well as an estimated outlook of the global electricity consumption up to the year 2035 considering the current energy policies [1]. To satisfy this demand we

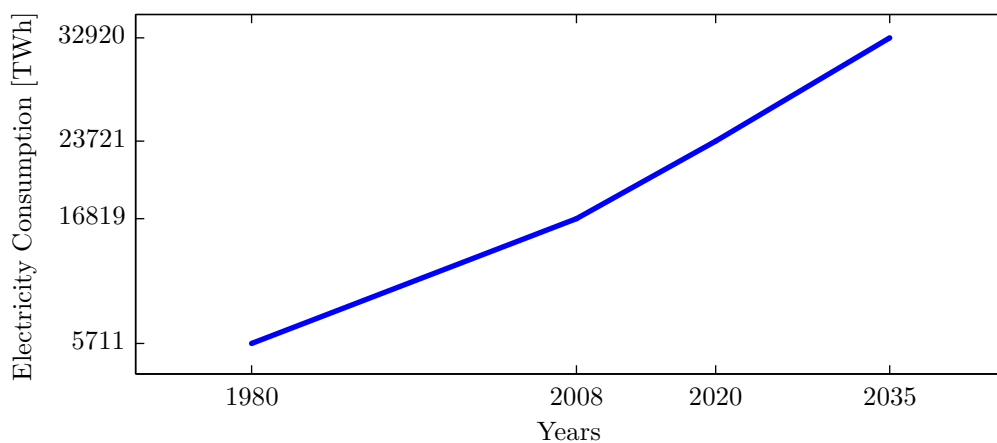


Figure 1.1: Global energy consumption past and outlook 1980-2035 regarding to current energy policies [1]

need to build new power plants, as well as increase the efficiency of existing grids and electrical equipment. Although the increasing demand and continuous expansion of electrification today, more than 1.4 billion (10^9) people worldwide still have no or only restricted access to electricity [1].

Since the discovery of electricity, significant efforts have been put into developing new energy sources. Most resources were and still are fossil fuels, such as coal, oil and natural gas as well as water and nuclear power. Due to various oil crises, a number of nuclear power plant incidents and the currently ongoing discussion about climate change, renewable energy resources become increasingly important and achieve more public acceptance and support. Wind and solar power are the two most commonly mentioned sources of renewable energy. In Fig. 1.2, we show the cumulatively installed capacity of wind power worldwide for the time frame from 1996 to 2010 [2] and it is going to continue to grow. With increasing wind and solar power generation the

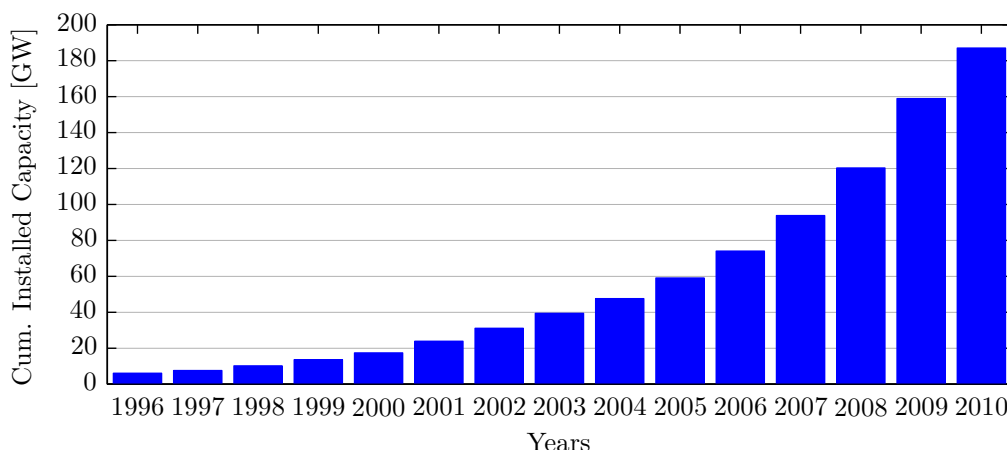


Figure 1.2: Global cumulative installed wind capacity 1996-2010 [2]

conventional transmission and distribution grid changes into a distributed system. In this system a lot of small and medium sized power plants are located on many different sites instead of only a few, large power plants. The type of power grid is changing from traditional distribution towards distributed generation. The direction of flow is no longer only from large power plants to households. A lot of smaller power plants are distributed throughout the grid and the power flow goes in all directions. The major problems about renewable energy resources like wind and solar are their volatility and their inaccurate predictability, as well as their intermittency. This problem does not only occur in the distribution grid, it also affects different voltage levels. Certainly, this effect grows bigger with the increasing power output of a wind power plant.

For power system stability the generated power has to match the consumed one as close possible at any time. This means the bigger wind farms are introduced to the grid, the more active work will be required to secure the reliability of the power grid. Better prediction accuracy as well as an increase in quantities of balance energy is required to avoid both, lack of energy, or overloading of branches. This energy comes from other power plants or storage units and has to be available immediately. On the other hand most of the connection lines are not dimensioned to deal with the maximum power output of connected power plants or wind farms. It does not occur often that the maximum power is produced. Therefore, it is economical cheaper to curtail this wind instead of building new lines with more capacity.

The energy of curtailed wind is irrecoverable. Bonneville Power Administration [3] in the United States estimated a total amount of 1 GWh for curtailed energy as of March 30, 2010. ERCOT, the Electric Reliability Council of Texas, USA [4], assumes that 500 MW to 2000 MW were curtailed daily between December 2008 and December 2009. Midwest ISO [5], another regional independent system operator in the U.S. published approximately 200 GWh of curtailed energy for the year 2009. Germany illustrated 74 GWh of curtailed wind energy [6] between 2004 and 2006.

Storage devices are required to avoid losing this energy. One could store this high-peak energy and transmit it whenever capacity is available on the lines. However, this means the electricity grid has to become more *intelligent* or a *smart* grid. A significant amount of effort is currently dedicated to invent such a *smart grid*. Stability of power supply is an absolute must in (or for) our future.

1.2 Problem Statement

Large amounts of electrical energy cannot be stored directly. We also cannot bottle, sack or bag electrical energy to transport it. This means electrical energy only can be transmitted in suitable amounts through wiring. For a stable and reliable grid it is essential that the sum of generated power is exactly equal to the sum of consumed power at any instant of time.

Whenever more power is generated than consumed, the frequency of the grid increases as a result of physical laws. On the other hand, if not enough power is produced the frequency goes down. Monitoring the frequency is the best way to observe the power balance of the grid. During normal operation, the bandwidth of frequency variations is within a few per mill because of continuous variations in the load. As soon as the deviation increases, the transmission grid operator has to counteract. This means that the power

generation has to be adjusted in accordance with the frequency trend. Equivalent changes to the load can also be applied by connecting or disconnecting some of the loads.

The load can be predicted with high accuracy based on historical measurements. However, imbalances between supply and demand are inevitable. There are different types of operating reserves to recover equilibrium. These reserves are ranging from only a few seconds for small amounts up to several minutes for larger quantities of energy. With the help of this balancing power the daily operation is guaranteed.

The accuracy of forecasting wind speed and solar radiation is not as precise as required. Wind energy is the kinetic energy of moving air. It is converted to power by turbines. This kinetic energy can be calculated based on a mass element dm and the wind velocity v of the volume of moving air that passes through the surface A [7]

$$dE = \frac{1}{2} dm v^2 = \frac{1}{2} \rho A v^3 dt. \quad (1.1)$$

Wind power that can be transformed into mechanical power to produce electricity can be derived to

$$p = \frac{1}{A} \frac{dE}{dt} = \frac{1}{2} \rho v^3. \quad (1.2)$$

The total wind power is proportional to the third power of wind velocity. This means the error between predicted and effective wind speed causes a deviation of the predicted power to the real power which is to the power of three higher than the error itself.

Currently, the amount of intermittent, renewable energies for electricity generation worldwide is quite small. There is enough operation reserve distributed throughout the grid to deal with the power and frequency variations. However, we need more energy generated by environmentally-friendly technologies to limit and counteract the climate change. Worldwide, we see a trend of significant expansion of renewable energies. The entire world is subject to these changes and considerations. A recent study from the Harvard University shows that the wind capacity available worldwide would be capable of covering more than 40 times the currently required consumption levels [8].

In order to ensure a stable and reliable power system in the future we have to improve the existing power grid to become a more efficient and intelligent system. It simply is not good enough to have sufficient operating reserves and to build new lines to transmit all the power generated. The grid has to become smart. It is required to control the power system in a more

flexible manner. Both, information and communication techniques play a decisive role. Actually, there are many additional approaches for smart grid applications.

One idea is to have distributed generation and storage so that power can be generated when the resource is available and be transmitted when the energy is required. With distributed storage, the energy could be stored at different locations starting at the site where the energy is generated. It could then be transferred whenever capacity is available on lines to other storage units closer to loads. In case of higher consumption than generation, the additional energy needed could be obtained from the closest storage. An additional advantage of such a system would also be that fact, that the power flow of the reserve power would not affect as many lines and long distances.

Another idea for smart grids is that certain types of electrical devices, such as washer and dryer can be turned on or off, pending on currently available energy. Using batteries of electric vehicles as storage units to have buffers close to the consumers would be another option for a distributed energy storage system.

The proper calculation of the required power flow on lines is essential ever since the deregulation of the electricity market. It will become even more important with the introduction of smart grids in the future. There are different reasons why calculating load flow for lines is absolutely essential. It is of utmost importance for planning purposes to predict the possible load flow distribution. It is required to find the trade-off between costs of building lines with higher or lower capacity and storage units especially when peak values do not occur very often.

The real time application and the planning phases have to be managed in other ways. These are two entirely different problems. Historically, one has primarily used Gaussian-distributed, independent, random variables for the load flow calculation. These variables were supposed to model the power injections. However, in recent years and especially due to the increasing introduction of wind power plants, non-gaussian distributed and correlated variables are of increasing importance. Correlation is an important factor for wind power plants, especially when they are geographically close to each other, because the wind affects all of them regarding to their distance.

All these problems are not only specific to North America or Europe. The entire world is subject to this changes and considerations. A lot of research and development is ongoing and much more is needed to have secure and reliable technologies for the smart grid applications in the future.

1.3 Contributions of this Thesis

World climate change is one of the most important and omnipresent topics for power systems today. It is very important to look at unsolved issues with regard to renewable energies and to find solutions for this issues, as well as more efficient technologies. Every development and improvement is a necessary step for a more environmentally-friendly energy system, starting from generation through transmission and continuing through storage to consumption.

The focus in our research is set on probabilistic load flow (PLF) for correlated wind power plant outputs. Since 1974, as Borkowska proposed the PLF-method for the first time [9], this method has been further developed [10]. Inputs for PLF simulations are probability density functions (PDFs) or cumulative distribution functions (CDFs) of power injections and loads. Outputs are also PDFs or CDFs of all branches. We decided to use PDF for our simulations. The relative frequency of occurrence of load values can be seen directly when using a PDF. The simulations are solved numerically by using random variables with a specific distribution. This numerical method is known as Monte Carlo Simulation.

The probability densities for wind park power outputs can often be described as a β -distribution [11, 12]. For two or more wind power plants, the influence of wind on these power plants can be modeled as a correlation between their power outputs with respect to their geographical distance to each other.

For PLF with correlated gaussian distributions and PLF without correlation, many different methods are available. Information on correlated and non-gaussian distributed characteristics are very rare and this requires more research activities.

For two or three wind park outputs with a specific β -distributed density function we can generate random variables with the required distribution and a desired correlation in the range from zero to one, if the correlation is possible. For two variables we can see how the distribution transforms from none to a total correlation and vice versa.

As second important part, besides the correlation, we introduced storage units into our model. On each bus where a wind power injection is connected, we located a storage unit. This storage facility will be used to optimize the power transfer from its generation to the load and avoid overloading the lines.

Additionally, with a storage unit at each injection bus we can also take certain line limits into account. We looked at a limit at the last line in a path. No consecutive limited lines are considered. We see then how the probability density changes on the line if a line limit is combined with storage units.

Chapter 2

Background

2.1 Power Flow

The power or load flow problem cannot be solved in an analytical manner due to non-linear equations. Iterative calculations and a number of simplifications are required. A number of different methods for electrical network analysis are available to accomplish this task. A well-known and often-used classification method is to categorize power flow models into AC and DC versions [13].

2.1.1 AC Power Flow

Precise power flow equations are used for AC power flow models and methods. These equations are non-linear. The solution for an AC power flow problem can be found by applying various methods using iterative calculations. Gauss-Seidel Iteration and Newton-Raphson methods are two of the best known options.

2.1.2 DC Power Flow

A DC power flow model or method can be used for an approximate solution of the power flow problem. Only active power is considered - no reactive power. DC models can be described by a set of linear equations and so the calculations are much faster [14–18].

After some approximations the linearized DC power flow equation for the active power flow can be derived to

$$P_{kl} = \frac{\theta_k - \theta_l}{x_{kl}}. \quad (2.1)$$

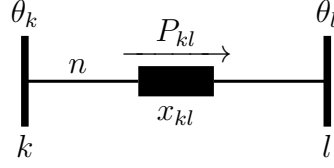


Figure 2.1: Basic 2 bus and 1 branch DC power flow model

This equation is equivalent to Ohm's Law applied to a resistor carrying a DC current as shown in Fig. 2.1. P_{kl} represents the DC current, θ_k and θ_l the DC voltages at the buses k and l and x_{kl} the resistance of the transmission line n .

For a larger system with buses $k, l = 1 \dots M$ and branches $n = 1 \dots Q$ the set of linear equations can be formulated into a matrix form

$$\mathbf{P} = \mathbf{B}' \boldsymbol{\theta} \quad (2.2)$$

where \mathbf{P} is the vector $(M - 1) \times 1$ of real power injections P_k at buses k , \mathbf{B}' is the nodal susceptance matrix $(M - 1) \times (M - 1)$ with elements

$$B'_{kl} = -\frac{1}{x_{kl}} \quad (2.3)$$

$$B'_{kk} = \sum_{l=1}^M \frac{1}{x_{kl}} \quad (2.4)$$

and $\boldsymbol{\theta}$ is the vector $(M - 1) \times 1$ of bus voltage angles θ_k . The slack bus has to be canceled out. For the power flow problem the nodal active power injections are known and the voltage angles at all buses (except for the slack bus - that is the reference bus with voltage angle $\theta = 0$) can be calculated as follows:

$$\boldsymbol{\theta} = (\mathbf{B}')^{-1} \mathbf{P}. \quad (2.5)$$

Multiplying the difference of voltage angles of the terminal buses k and l of a branch n with the inverse of the branch reactance leads to the power flow on this line (2.7).

$$\theta_{kl} = \theta_k - \theta_l \quad (2.6)$$

$$P_{kl} = \frac{1}{x_{kl}} \cdot \theta_{kl} \quad (2.7)$$

2.2 Power Transfer Distribution Factor

When using a DC power flow model, an incremental method for calculating power flow can be applied. With DC Power Transfer Distribution Factors

(PDTFs) a relative change in power flow on a specific line due to a relative change in power injection at a particular bus can be derived. The calculation is based on DC power flow equations. From (2.2) the incremental version is as follows:

$$\Delta \mathbf{P} = \mathbf{B}' \Delta \boldsymbol{\theta}. \quad (2.8)$$

After transformation we obtain

$$\Delta \boldsymbol{\theta} = \mathbf{X} \Delta \mathbf{P} \quad (2.9)$$

where \mathbf{X} is the reactance matrix, the inverse of the susceptance matrix \mathbf{B}' extended with a row and a column of zeros at the position where the slack bus is located like

$$\mathbf{X} = \begin{pmatrix} X_{11} & \cdots & X_{1(j-1)} & 0 & X_{1(j+1)} & \cdots & X_{1M} \\ \vdots & \ddots & \vdots & \vdots & \vdots & \ddots & \vdots \\ X_{(j-1)1} & \cdots & X_{(j-1)(j-1)} & 0 & X_{(j-1)(j+1)} & \cdots & X_{(j-1)M} \\ 0 & \cdots & 0 & 0 & 0 & \cdots & 0 \\ X_{(j+1)1} & \cdots & X_{(j+1)(j-1)} & 0 & X_{(j+1)(j+1)} & \cdots & X_{(j+1)M} \\ \vdots & \ddots & \vdots & \vdots & \vdots & \ddots & \vdots \\ X_{M1} & \cdots & X_{M(j-1)} & 0 & X_{M(j+1)} & \cdots & X_{MM} \end{pmatrix}. \quad (2.10)$$

In this case, bus j is the slack. Both vectors $\Delta \boldsymbol{\theta}$ and $\Delta \mathbf{P}$ also include slack bus information.

The power transfer distribution factors $\psi_{n,i}$ corresponding to branch n and power change on bus i can be formulated as

$$\psi_{n,i} = \frac{dP_n}{dP_i} \quad (2.11)$$

where dP_n represents the variation in power flow on branch n and dP_i stands for the relative change of power injection or consumption at bus i .

After some mathematical transformations the PTDFs can be calculated by using

$$\psi_{n,i} = \frac{1}{x_{kl}} (X_{ki} - X_{li}) \quad (2.12)$$

where X_{ki} and X_{li} are elements from the reactance matrix \mathbf{X} . PTDFs and similar distribution factors are discussed in detail in [16–26].

2.3 Methods for Probabilistic Power Flow

Probabilistic load or power flow calculations are analytical alternatives to deterministic techniques of solving the power flow equations. The probabilistic nature of input and output parameters is the key feature. Power injections and loads are modeled by random variables. Probability density functions or cumulative distribution functions are used to describe the probabilistic nature of these parameters.

The probabilistic load flow method was introduced by Borkowska for the first time in 1974 [9]. Prior to that introduction only deterministic methods were known [27, 28]. Since 1974 various techniques for solving the probabilistic load flow problem were developed and the research and development is still in progress. Initial researches only used the DC load flow method. Just shortly thereafter, the first papers using the AC load flow were published. Overviews and summaries, including and comparing the different methods were also published [29, 30].

Another statistical method similar to probabilistic load flow is the stochastic load flow [31–34]. A stochastic load flow analysis uses a state estimator-type algorithm. It is an extremely fast technique, but it only can handle probability density functions of the Gaussian type. An option for non-Gaussian probability distributions is discussed in [35]. We focused on probabilistic load flow only, but some of the methods described below are combining probabilistic and stochastic load flow models.

Borkowska [9], as well as Allan and many others [36–49] used the convolution technique. The probability density of the sum of two independent random variables is the convolution of their density function [50]. With this technique the line flow can be calculated by convoluting the density functions of the power injections. The limitation is that each generation and load is required to be independent from each other.

Some approaches to handle dependencies were discussed. In these papers, discrete or Gaussian distributions for nodal power generation or loads were used. There are different ways to calculate the convolution. One of the two main calculation methods is the classical and well-known convolution integral. The other one is through fast Fourier transformations algorithm.

For density functions with Gaussian shape a solution of the convolution exists in closed form (the result is also a Gaussian distribution [51]), but in general a conversion to a discrete density function and a numerical computation is necessary. This fact and the requirement of independence for the random variables make this technique obsolete for our research.

Different methods use a higher level of statistical techniques. Two very important elements of such probabilistic power flow methods are known as

moments [52–54] and cumulants [54, 55] in probability theory and statistics. Statistical moments describe the shape of a distribution. The first four moments are well known. The first moment is the mean, the second is variance, the third is skewness and the fourth is kurtosis.

An alternative to statistical moments are cumulants. Cumulants are a set of quantities to approximate the shape of a distribution. A distribution is better described by its cumulants than by its moments [56]. The cumulants are related to the statistical moments and can be calculated by a recursion formula using the statistical moments as a basis.

Several methods or combinations of methods using moments or cumulants do exist. A Taylor series to obtain moments is used in [57]. A combination of moments and cumulants extended by a mathematical method called Von Mises [58] is used in [59] and a mix of method of cumulants and Von Mises is applied to stochastic load flow in [60].

The cumulant method is often combined with the Gram-Charlier series expansion theory. Edgeworth series and Gram-Charlier series are used to approximate the probability distribution [55, 61]. The Gram-Charlier series is used more often to build a density function from cumulants in a probabilistic power flow computation.

The interpretation of moments or cumulants by the Gram-Charlier series to solve a probabilistic power flow problem is explained and discussed in [62–64]. The cumulant method in combination with Gram-Charlier series is applied to an optimal power flow problem in [65] using Gaussian and Gamma distributions. An enhancement of this cumulant method is presented in [66]. For the enhancement discussed in this paper only a Gaussian distribution is used.

Many other researchers used this concept of combining cumulants and Gram-Charlier series to rebuild probability density functions. In [26, 67, 68] network configuration uncertainties or vulnerability assessment [69], as well as reactive power control [70] are discussed based on this method. Transfer capability analysis can also be performed through probabilistic load flow using cumulants [71] or moments [72] in combination with Gram-Charlier series expansion.

Gram-Charlier series are a great tool to approximate Gaussian distributions, especially in cases where data significantly differ from a normal distribution, higher orders of moments and cumulants are needed for a meaningful approximation. For non-Gaussian distributions this method has some convergence problems.

Another approach to load flow calculation was proposed in [73]. This method uses a point estimation method [74, 75] to achieve a better fitting of the probability density function from statistical moments. A good summary

including different point-estimation methods and their comparison to power flow calculation can be found in [76]. A two-point estimation method was also used in [77, 78]. The point-estimation method was extended in [79] to account for dependencies among random variables.

With the Cornish-Fisher expansion series [61, 80] a technique with better convergence properties than Gram-Charlier series for approximation of non-Gaussian density functions was found. Many researchers applied the method of combined cumulants and Cornish-Fisher expansion to power flow problems [81–84]. Usaola also discussed dependencies among input random variables [85, 86].

In [85] he proposed a technique called Enhanced Linear Method. For injection of the wind power, he uses dependent, β -distributed random variables. Loads are modeled by dependent or independent normal variables with a given correlation matrix. To generate the correlated random variables in [85, 86] Usaola uses a method based on the inverse transformation of a uniform distribution, see Section 2.7.1 for details.

Cornish-Fisher series are usually much better than Gram-Charlier series for fitting non-Gaussian distributions, but the convergence properties are difficult to demonstrate and the complexity of this mathematical problem is not yet completely solved [80].

A different approach is the fuzzy power flow [87, 88]. Load and generation uncertainties are modeled as fuzzy numbers instead of random variables. This is important in cases, where no statistical information is available – so this is no probabilistic load flow method. An overview about the fuzzy power flow is provided in [89].

The oldest and best known method for probabilistic load flow is Monte Carlo simulation [90]. Monte Carlo is a numerical technique. A result can be computed by repeated, random sampling. Many of the methods mentioned above are using Monte Carlo methodology to verify, or to compare their computation results. Monte Carlo also can be combined with different approaches, or the calculation can be finalized by using this method.

In [91, 92], Monte Carlo is applied to multi-linearized load flow equations. A combination of Markov Chains and Monte Carlo is presented in [93]. For transmission planning and complex power systems, Monte Carlo is applied in [94, 95] and the wind generation cost is also considered in [96].

In addition, the correlations between loads and generation in combination with wind power is considered in [97]. It is taken into consideration from -1 to 1 using Spearman rank correlation coefficient. In this paper the correlated random variables are also uniformly distributed and have to be transformed. The probability density function of the wind power injection is derived from the wind speed distribution. If the wind speed is Weibull-distributed, than

the distribution of the wind turbine is another Weibull distribution, otherwise there is no closed form for the density function.

Using the Monte Carlo method, there are virtually no limitations for assumptions of the simulation process. It is an universal technique and can be applied to almost all problems of probabilistic load flow. It can compute a result even in cases, where other methods are restricted. However, it might be a rather time consuming process. For very complex problems the major disadvantage could be the time needed to finish the computation and the required computational effort.

Another method was proposed in [98]. It is called the sequential time-series probabilistic load flow approach. In this paper a DC load flow model was used and a discretization to the density function was applied. This discretization procedure was called multi-dimensional clustering. The computation was performed by linear programming optimization.

We reviewed many different ways to compute a solution for a probabilistic power flow problem. Advantages, disadvantages and limitations of different techniques were discussed. Most of these methods used Gaussian distributed random variables. Correlations among loads and generation are discussed and considered only in a few papers. The research for correlated random variables with any distribution is still in progress.

2.4 Power Output Characteristics of Wind Farms

The distribution of wind turbine output depends on the wind speed distribution and can be calculated from it. Wind turbine power output, as well as using its relationship to the wind speed is discussed in [81, 83]. The power output distribution of an entire wind farm is a combination of many single wind turbine power output distributions.

The wind farm power output distribution for a farm with 200 2 MVA wind turbines is shown in [96]. This distribution is an extrapolation of the energy conversion from a Weibull wind speed distribution of one wind turbine up to a total of 200 equal turbines – no restrictions or limitations were considered.

The probability density function of a wind power output for large systems was investigated by Louie [11, 12]. The output distribution for larger areas of wind production typically has a β -characteristic. Some of these output distributions are similar to the one discussed in [96], except for the peak at maximum power.

The mix of wind turbines in the greater areas discussed by Louie includes

turbines of different types and nominal ratings. An output distribution of a wind farm mostly is the combination of curtailed and uncurtailed wind turbine production distributions due to power injection restrictions or connection line limits.

2.5 Constitutive Probability Distributions

In this section we introduce the basics and properties of the Beta and the elementary Gamma distribution as well as their relationship.

2.5.1 γ -Distribution

The standard γ -distribution [99] on the interval $[0, \infty)$ is:

$$f(x, \alpha, \lambda) = \frac{\lambda^\alpha}{\Gamma(\alpha)} x^{\alpha-1} \exp^{-\lambda x} \quad x \in [0, \infty); \alpha, \lambda > 0 \quad (2.13)$$

with Gamma function:

$$\Gamma(\alpha) = (\alpha - 1)! \quad (2.14)$$

where α is the shape parameter and λ is the scale parameter. The expected value or mean can be calculated like

$$\mu = \alpha\lambda \quad (2.15)$$

and the variance as

$$\sigma^2 = \alpha\lambda^2. \quad (2.16)$$

2.5.2 β -Distribution

The standard β -distribution [100] on the interval $[0, 1]$ is:

$$f(x, \alpha, \beta) = \frac{1}{B(\alpha, \beta)} x^{\alpha-1} (1-x)^{\beta-1} \quad x \in [0, 1]; \alpha, \beta > 0 \quad (2.17)$$

with Beta function

$$B(\alpha, \beta) = \frac{\Gamma(\alpha)\Gamma(\beta)}{\Gamma(\alpha + \beta)} = \int_0^1 u^{\alpha-1} (1-u)^{\beta-1} du \quad (2.18)$$

where α and β are real shape parameters of the distribution. Both shape parameters can be calculated if mean μ and variance σ^2 are known for a

specific distribution by using

$$\alpha = \mu \left(\frac{\mu(1-\mu)}{\sigma^2} - 1 \right) \quad (2.19)$$

$$\beta = (1-\mu) \left(\frac{\mu(1-\mu)}{\sigma^2} - 1 \right). \quad (2.20)$$

These equations can be derived from equations for the expected value

$$\mu = \frac{\alpha}{\alpha + \beta} \quad (2.21)$$

and the variance

$$\sigma^2 = \frac{\alpha\beta}{(\alpha + \beta)^2 (\alpha + \beta + 1)}. \quad (2.22)$$

We obtain the β -distribution for the interval $[a, b]$:

$$f(x', a, b, \alpha, \beta) = \frac{1}{B(a, b, \alpha, \beta)} (x' - a)^{\alpha-1} (b - x')^{\beta-1} \quad x' \in [a, b]; \quad \alpha, \beta > 0 \quad (2.23)$$

with Beta function

$$B(a, b, \alpha, \beta) = \frac{\Gamma(\alpha)\Gamma(\beta)}{\Gamma(\alpha + \beta)} (b - a)^{\alpha+\beta-1} = \int_a^b (u - a)^{\alpha-1} (b - u)^{\beta-1} du \quad (2.24)$$

by applying the transformation

$$x = \frac{x' - a}{b - a} \quad (2.25)$$

to (2.17).

2.6 Linear Correlation

Dependencies between random variables can be formulated in different ways, measures, or functions. One measure of dependency is the covariance [52]

$$\text{Cov}_{X,Y} = \sigma_{X,Y} = \text{E}[(X - \text{E}[X])(Y - \text{E}[Y])]. \quad (2.26)$$

The covariance is unit dependent and this can be the problematical dependency of the application. The covariance is positive, if the random variables X and Y have a linear relationship and the same direction. The covariance is negative, if the linear relationship is in reverse direction.

For a unit independent measure of dependency, the covariance can be divided by the product of the standard deviations of the random variables. This fraction is called the Pearson correlation coefficient or the coefficient of linear correlation [52].

$$\text{Corr}_{X,Y} = \rho_{X,Y} = \frac{\sigma_{X,Y}}{\sigma_X \sigma_Y}. \quad (2.27)$$

The correlation coefficient has the same sign as the covariance. Because of Cauchy–Schwarz inequality, following can be formulated

$$|\sigma_{X,Y}| \leq \sigma_X \sigma_Y. \quad (2.28)$$

The range of the correlation coefficient is bounded to $-1 \leq \text{Corr}_{X,Y} \leq 1$. If the correlation is zero, the random variables are uncorrelated, but they do not have to be independent. On the other hand, independent random variables are definitely not correlated.

This correlation coefficient is the one most commonly used. Others are for instance Spearman’s rank correlation coefficient and Kendall’s rank correlation coefficient. Rank correlation coefficients work differently. If an increase of X always comes with an increase of Y , the correlation would be considered perfect. However, it is not required that all single values are lying on a straight line, as it is for the Pearson coefficient.

Another way to describe the relationship between random variables are copulas [101]. A copula is a function which describes any type of relationship between random variables. It is a much more complex method to describe dependencies.

A good overview of the different kinds of dependencies of random variables, or correlated random variable generation methods and algorithms can be found in [102].

2.7 Correlated Random Variables

There are different ways of generating correlated β -distributed random variables. In this section we give a short overview of different ways to produce such random variables.

2.7.1 Uniformly Distributed and Correlated Random Variables Transformed to Desired Distribution

The classical way to produce correlated random variables with a required distribution is to start with generation of uniformly distributed random variables within the interval (0,1) and the desired correlation. These random

variables are then transformed to random variables with the desired distribution. This method is used and explained in [86, 103, 104] for generating β -distributed random variables.

With this conversation the correlation changes depending on the target distribution and the range of the distribution. Some adjustments might be necessary to obtain the desired correlation. In addition, sometimes there are restrictions for the range of correlation.

2.7.2 Dirichlet Distribution

Mario Catalani describes a method for generating positively correlated random variables with β -distribution in [105]. He uses the fact that the marginals of a Dirichlet distribution are beta variates.

Basically, this method uses the nature of composition a β -distribution from two or more γ -distributions. Based on the Dirichlet distribution a correlation among beta variates exists. This method has restrictions with respect to the shape parameters of β -distributions. One limitation is, that the sum of the parameters has to be equal for all β -distributions like

$$\alpha_1 + \beta_1 = \alpha_2 + \beta_2. \quad (2.29)$$

2.7.3 Shared Random Variables for Correlation

This method uses similar properties of β -distributions as the Dirichlet method we discussed in Section 2.7.2 and was proposed by Magnussen [106]. The composition of a β -distribution from two or more γ -distributions is the first basic idea of his method. The second essential step is, to use the well-known additivity of γ -distributed random variables.

By combining the additivity and the composition as fundamental third step, Magnussen created a β -distribution with parameters α and β , where each shape parameter is a sum of two specific sub-parameters. To obtain a certain correlation for two β -distributions, he shared one of these two sub-parameters per shape parameter between both compositions. To share a sub-parameter means to share a γ -distributed random variable.

Magnussen used parameters $\alpha_1 = 1, 3, 5, \dots, 31$ and $\beta = \alpha_1, \alpha_1 + 10, \alpha_1 + 20, \dots, \alpha_1 + 100$. He also stated, that a bias occurs due to the cutting of the series expansion. The smaller the parameters α and β , the larger the bias. For wind applications the parameters for β -distributions are normally smaller than 3, see Section 2.4. For such small values, a bias of more than 10 % to 20 % occurs.

Chapter 3

Methodology of Correlation

For our work we decided to use and enhance the method from Magnussen as mentioned in Section 2.7.3. We noticed that this method offers significant possibilities. Therefore, we adopted it to fit our requirements. The main issue was the calculation of the shared variables and we developed a method that was usable for our simulations.

3.1 Application of Available Methods

Let U_1 and U_2 be two γ -distributed random variables and V a β -distributed one. The composition V out of U_1 and U_2 is calculated like

$$V = \frac{U_1}{U_1 + U_2}. \quad (3.1)$$

$$\left. \begin{array}{l} U_1 \sim \mathcal{G}(\gamma_1, \lambda) \\ U_2 \sim \mathcal{G}(\gamma_2, \lambda) \end{array} \right\} V \sim \mathcal{B}(\gamma_1, \gamma_2) \quad (3.2)$$

The symbol \sim stands for *distributed as* and $\mathcal{G}(\gamma, \lambda)$ or $\mathcal{B}(\gamma_1, \gamma_2)$ denotes a γ -distribution with shape parameter γ and scale parameter λ , and a β -distribution with shape parameters γ_1 and γ_2 , respectively. As shown above, the shape parameter of each γ -distribution turns into a shape parameter of the composed β -distribution. The scale parameters have to be equal.

The sum of two γ -distributed random variables also results in a random variable W_1 that is γ -distributed, like

$$W_1 = U_1 + U_2. \quad (3.3)$$

$$\left. \begin{array}{l} U_1 \sim \mathcal{G}(\gamma_1, \lambda) \\ U_2 \sim \mathcal{G}(\gamma_2, \lambda) \end{array} \right\} W_1 \sim \mathcal{G}(\gamma_1 + \gamma_2, \lambda) \quad (3.4)$$

The shape parameter of the result is the sum of the shape parameters of each summand.

In his method, equations (3.1) and (3.3) are combined like

$$V = \frac{W_1}{W_1 + W_2} = \frac{U_1 + U_2}{U_1 + U_2 + U_3 + U_4}. \quad (3.5)$$

$$\left. \begin{array}{l} U_1 \sim \mathcal{G}(\gamma_1, \lambda) \\ U_2 \sim \mathcal{G}(\gamma_2, \lambda) \\ U_3 \sim \mathcal{G}(\gamma_3, \lambda) \\ U_4 \sim \mathcal{G}(\gamma_4, \lambda) \end{array} \right\} V \sim \mathcal{B}(\gamma_1 + \gamma_2, \gamma_3 + \gamma_4) \quad (3.6)$$

Each shape parameter of the β -distribution is split into two parts

$$\alpha = \gamma_1 + \gamma_2 \quad (3.7)$$

$$\beta = \gamma_3 + \gamma_4. \quad (3.8)$$

To achieve a certain correlation among β -distributed random variables, Magnussen shared γ -distributed random variables among their composition calculation. For two correlated random variables Y_1 and Y_2 this looks like

$$Y_1 = \frac{X_1 + X_a}{X_1 + X_a + X_2 + X_b} \quad (3.9)$$

$$Y_2 = \frac{X_3 + X_a}{X_3 + X_a + X_4 + X_b}. \quad (3.10)$$

X_a and X_b are shared variables added to obtain the desired correlation. These variables are calculated from all shape parameters and their respective correlation. Depending on the correlation factor the shape parameters for the shared random variables have different values. Magnussen split α and β in a specific way by calculating a first-order Taylor series approximation to the covariance between Y_1 and Y_2 .

We started applying this method to our research work and generated correlated β -distributed random variables Y_1 and Y_2 . To analyze the full range of correlation from 0% to 100% in 10% steps we composed each combination of corresponding, γ -distributed random variables and checked their actual correlation.

From the results of our simulations with respect to this method with shape parameters $\alpha_1 = 0.87$ and $\beta_1 = 1.23$ for the first and $\alpha_2 = 0.87$ and $\beta_2 = 1.23$ for the second β -distribution, it can be verified that the shape parameters α and β are too small for this method to achieve the desired

correlations. The values of the achieved correlations are a slightly more than half of what they should be (e.g. 26 % instead of 50 % or 55 % instead of 100 %). Tests with larger parameters achieved the right correlation levels.

In the derivation of this method, Magnussen used a first-order Taylor series expansion. This approximation may have caused the bias. A bias larger than 10 % may be restricted to β -distributions with near exponential or exponential-types. For smaller values of parameters α and β the bias is larger. Therefore, this method cannot be used for small parameters.

3.2 Adaptation for Better Correlation

However, we appreciated the option of using a shared random variable to control the correlation. Our work focused on the issue that the achievable correlation gets closer to the target correlation. We worked on a method to derive the shape parameters γ_a and γ_b for the shared random variables X_a and X_b .

We developed a method to achieve a better method to calculate correlation for small values of shape parameters. Applying a marginal correlation allows us to achieve a perfect correlation. This is shown in Section 3.4.

We define the parameters α_1, β_1 and α_2, β_2 in general as follows:

$$\alpha_1 = \alpha_\rho \cdot a_1 + a_{1,0} \quad (3.11)$$

$$\beta_1 = \beta_\rho \cdot b_1 + b_{1,0} \quad (3.12)$$

$$\alpha_2 = \alpha_\rho \cdot a_2 + a_{2,0} \quad (3.13)$$

$$\beta_2 = \beta_\rho \cdot b_2 + b_{2,0} \quad (3.14)$$

where α_ρ and β_ρ are shared factors, and a_1, b_1, a_2, b_2 are scale parameters for the correlation and $a_{1,0}, b_{1,0}, a_{2,0}, b_{2,0}$ are independent terms.

Further, we define

$$\alpha_\rho = \max(\alpha_1, \alpha_2) \quad (3.15)$$

$$\beta_\rho = \max(\beta_1, \beta_2) \quad (3.16)$$

for positive correlation, and

$$\alpha_\rho = \max(\alpha_1, \beta_2) \quad (3.17)$$

$$\beta_\rho = \max(\beta_1, \alpha_2) \quad (3.18)$$

for negative correlation. To archive the proper level of correlation we set the scale parameters a_1, b_1, a_2, b_2 equal to the correlation factor ρ . Independent parameters are assigned to the shape parameters of the non-shared γ -distributed random variables $\gamma_1, \gamma_2, \gamma_3, \gamma_4$.

For a positive correlation with correlation factor ρ between Y_a and Y_b we consequently calculated our shape parameters γ_a and γ_b like

$$\gamma_a = \rho \cdot \max(\alpha_1, \alpha_2) \quad (3.19)$$

$$\gamma_b = \rho \cdot \max(\beta_1, \beta_2). \quad (3.20)$$

For negative correlation the calculation is as follows

$$\gamma_a = \rho \cdot \max(\alpha_1, \beta_2) \quad (3.21)$$

$$\gamma_b = \rho \cdot \max(\beta_1, \alpha_2). \quad (3.22)$$

Using these parameters, we obtain random variables with distributions

$$X_a \sim \mathcal{G}(\gamma_a, \lambda) \quad (3.23)$$

$$X_b \sim \mathcal{G}(\gamma_b, \lambda). \quad (3.24)$$

The parameter calculation of all independent non-shared γ -distributed random variables for positive correlation is performed by

$$\gamma_1 = \alpha_1 - \gamma_a \quad (3.25)$$

$$\gamma_2 = \beta_1 - \gamma_b \quad (3.26)$$

$$\gamma_3 = \alpha_2 - \gamma_a \quad (3.27)$$

$$\gamma_4 = \beta_2 - \gamma_b. \quad (3.28)$$

For negative correlation, the parameter calculation of γ_3 and γ_4 is different

$$\gamma_3 = \alpha_2 - \gamma_b \quad (3.29)$$

$$\gamma_4 = \beta_2 - \gamma_a. \quad (3.30)$$

The corresponding random variables can be generated by

$$X_1 \sim \mathcal{G}(\gamma_1, \lambda) \quad (3.31)$$

$$X_2 \sim \mathcal{G}(\gamma_2, \lambda) \quad (3.32)$$

$$X_3 \sim \mathcal{G}(\gamma_3, \lambda) \quad (3.33)$$

$$X_4 \sim \mathcal{G}(\gamma_4, \lambda). \quad (3.34)$$

The composition of the β -distributed random variables Y_1 and Y_2 is the same as (3.9) and (3.10)

$$Y_1 = \frac{X_1 + X_a}{X_1 + X_a + X_2 + X_b}$$

$$Y_2 = \frac{X_3 + X_a}{X_3 + X_a + X_4 + X_b}.$$

A flow chart of our algorithm for parameter calculation can be found in Fig. 3.1.

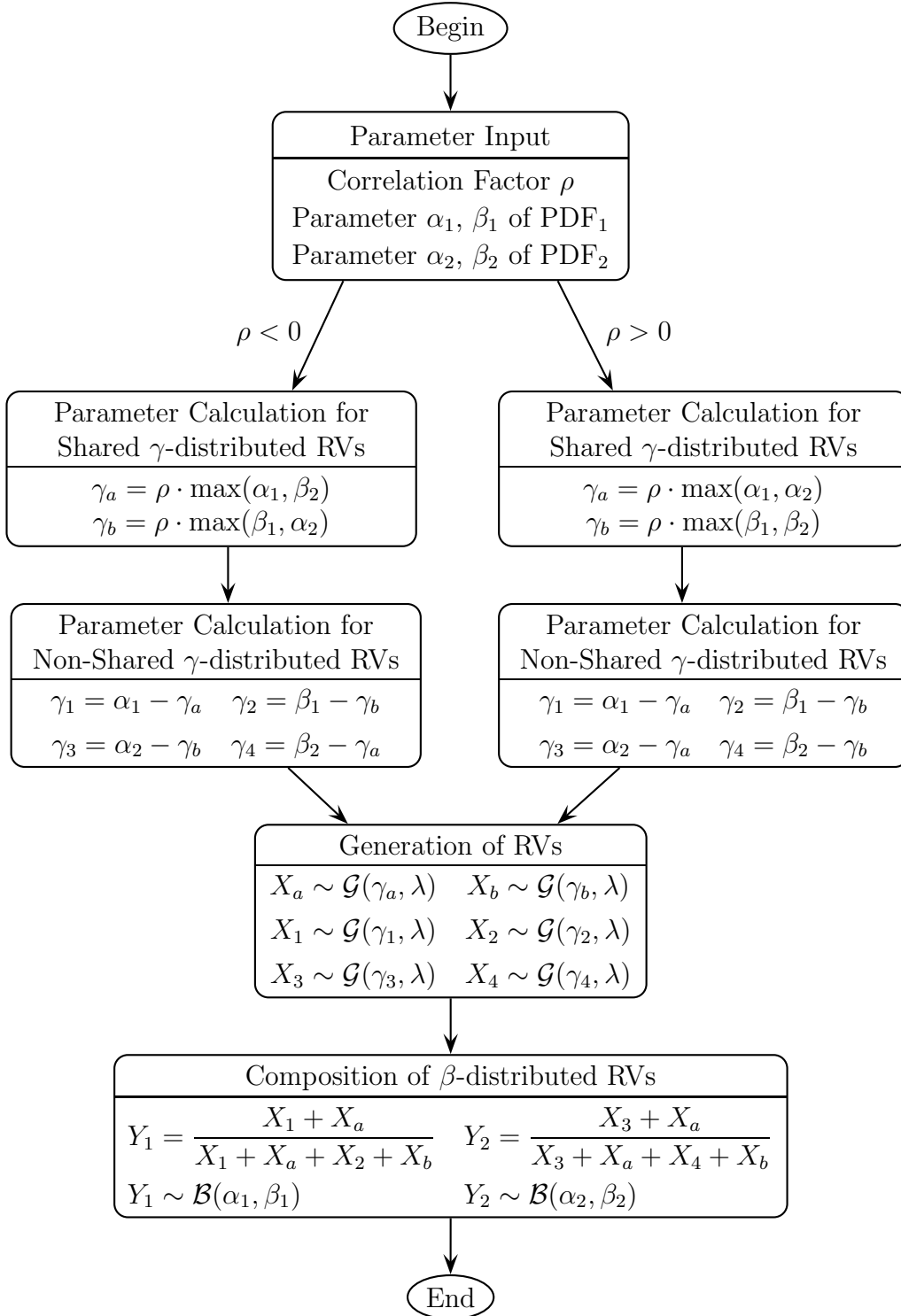


Figure 3.1: Flow chart of parameter calculation algorithm

3.3 Summation of Two Random Variables

For testing purposes we simulated the summation of two β -distributed random variables at different levels of correlation. We used steps of 10 % from 0 % to 100 % correlation. These simulations were equivalent to the superposition of different flows at one branch in the power flow application. The total power flow corresponds to Z , and

$$Z = Y_1 + Y_2 \quad (3.35)$$

with $Y_1 \sim \mathcal{B}(\alpha_1, \beta_1)$ and $Y_2 \sim \mathcal{B}(\alpha_2, \beta_2)$.

We generated the γ -distributed random variables using the *MATLAB* `gamrnd` function from the statistics toolbox. Each set of generated random variables consists of a total of one million samples. All six random variables are generated this way for each level of correlation and then both β -distributed random variables are composed out of this pool, as described in the previous section. All calculations have a resolution of 0.5 % steps.

The convolution is performed by the elementary math function `conv` in *MATLAB*. For convolution method the density functions with beta characteristics are generated by the `betapdf`-function of the statistics toolbox. The first value is infinity and is limited to the value one. For the case of identical variables, the random variables are generated by the same algorithm than for any other correlation, using the composition of random variables generated by the `gamrnd`-function.

First, we tested a configuration with two identical β -distributions. These distributions have of course same shape parameters $\alpha_1 = \alpha_2 = 0.87$ and $\beta_1 = \beta_2 = 1.23$. The simulation result can be found in Fig. 3.2. The different colored lines are representing different levels of correlation.

Additionally, the light blue curve shows the calculation result of the convolution of the two probabilistic density functions of independent random variables. The black curves represent the original source density functions. In this case both distributions are congruent and quite the same than a 100 % correlation. With higher resolution they would also coincide.

The achieved correlation is reasonably good but it still has a small bias of smaller than 20 %. The smaller the correlation the higher the bias. Now, we can see the transformation of the sum from the case of independent random variables represented by the dark blue curve to totally correlated or identical variables shown as the brown curve.

In Fig. 3.3, we show the simulation result for an opposite shape, but same parameters for the β -distributions with positive correlation. This proves, that the shape parameters are contrary with $\alpha_1 = \beta_2 = 0.87$ and $\alpha_2 = \beta_1 = 1.23$. With this difference in shape only about 77 % of correlation is possible. The

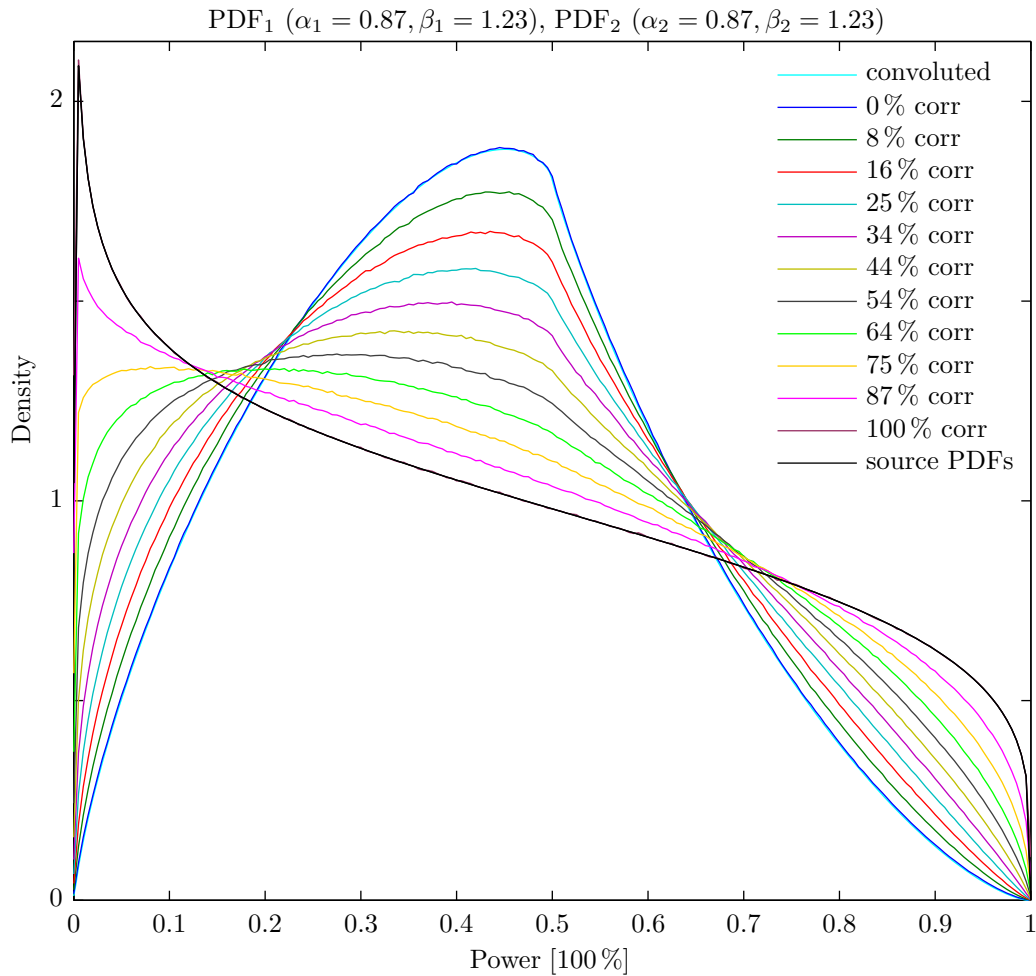


Figure 3.2: Positive correlation and distributions with the same shape

term *NaN* stands for *Not a Number* and this means that no valid result during the simulation could be achieved.

In Fig. 3.4 and Fig. 3.5, the same simulations are shown, but with negative correlation. Fig. 3.4 shows identical shapes of distributions, so the black curves are congruent again and in Fig. 3.5 opposite shapes can be found.

Here, of course, a totally correlation is possible for contrary shapes. For identical shapes only about 77% can be achieved. A correlation of 80%, 90% or 100% is not possible at all in this case. For a total correlation, the density function is only a peak at zero.

For contrary shapes the bias is a little bit different. It is max. 10% and can be smaller or larger than the desired value while the bias for distributions with same shapes is only smaller.

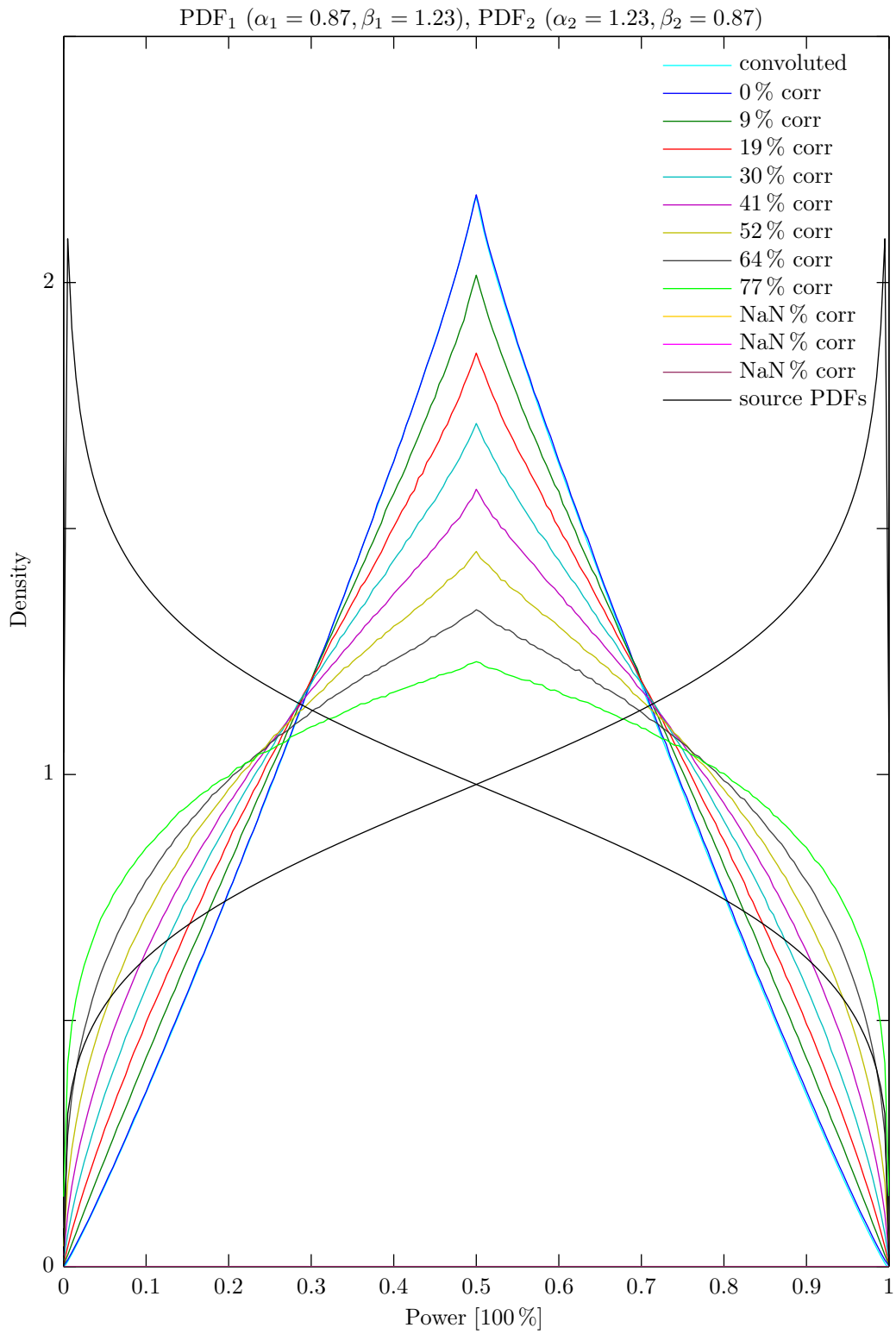


Figure 3.3: Positive correlation and distributions with contrary shapes

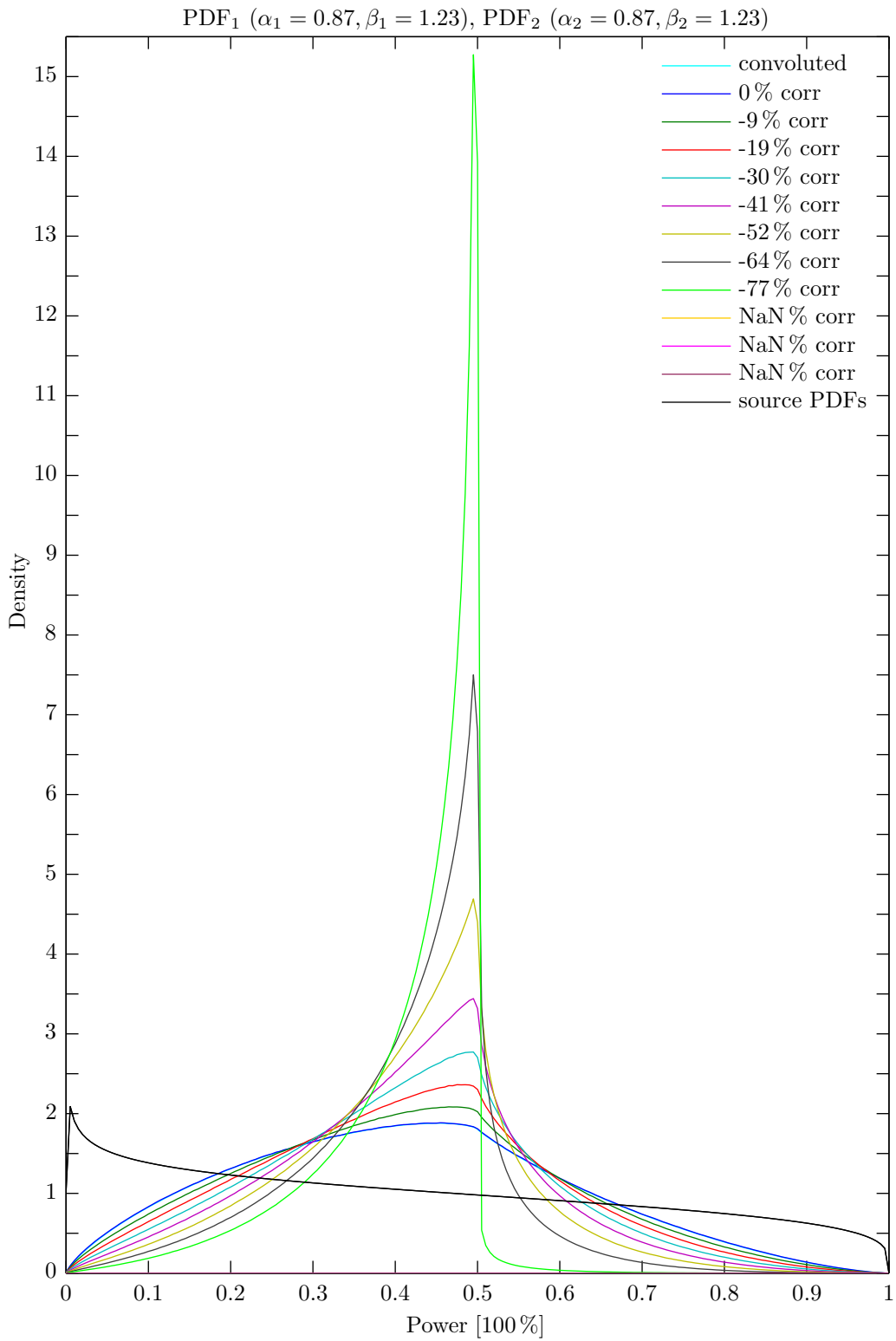


Figure 3.4: Negative correlation and distributions with the same shape

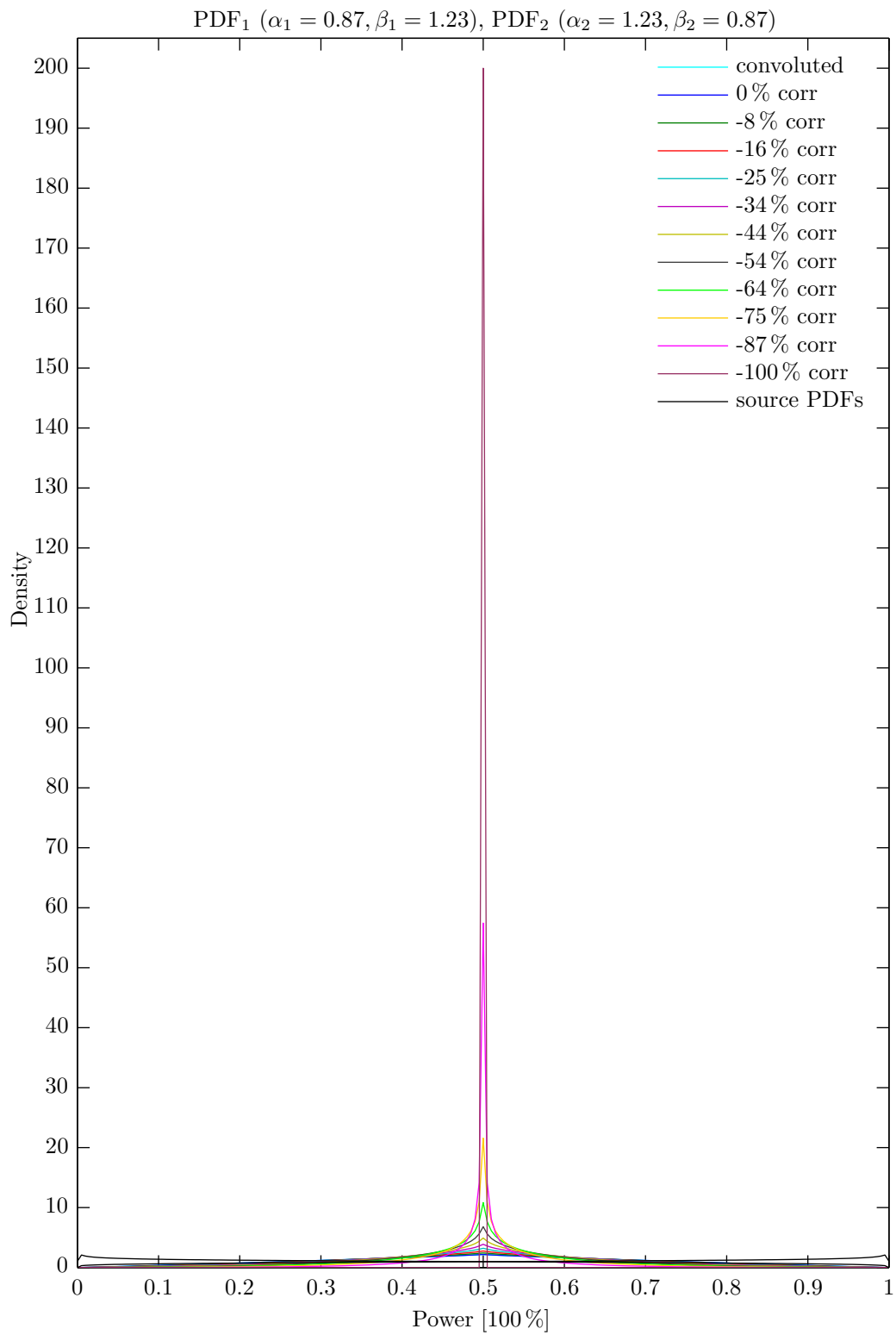


Figure 3.5: Negative correlation and distributions with contrary shapes

3.4 Linearity Error Compensation

In our research we especially focused on the case of β -distributions with similar shapes and positive correlation. We worked towards perfecting the random variable generation method proposed in section 3.1. Negative correlation as well as shapes with parameters where $\alpha > \beta$ are not that important for the application to wind farms.

We start our analysis for β -distributions with exact same parameters. In this case we can reach any correlation in the full range from 0 to 100 %. For the following considerations we used the parameters $\alpha_1 = \alpha_2 = 0.87$ and $\beta_1 = \beta_2 = 1.23$. In Fig. 3.6, we see a red straight line which represents a perfect correlation. The green, sagging curve shows the measured correlation

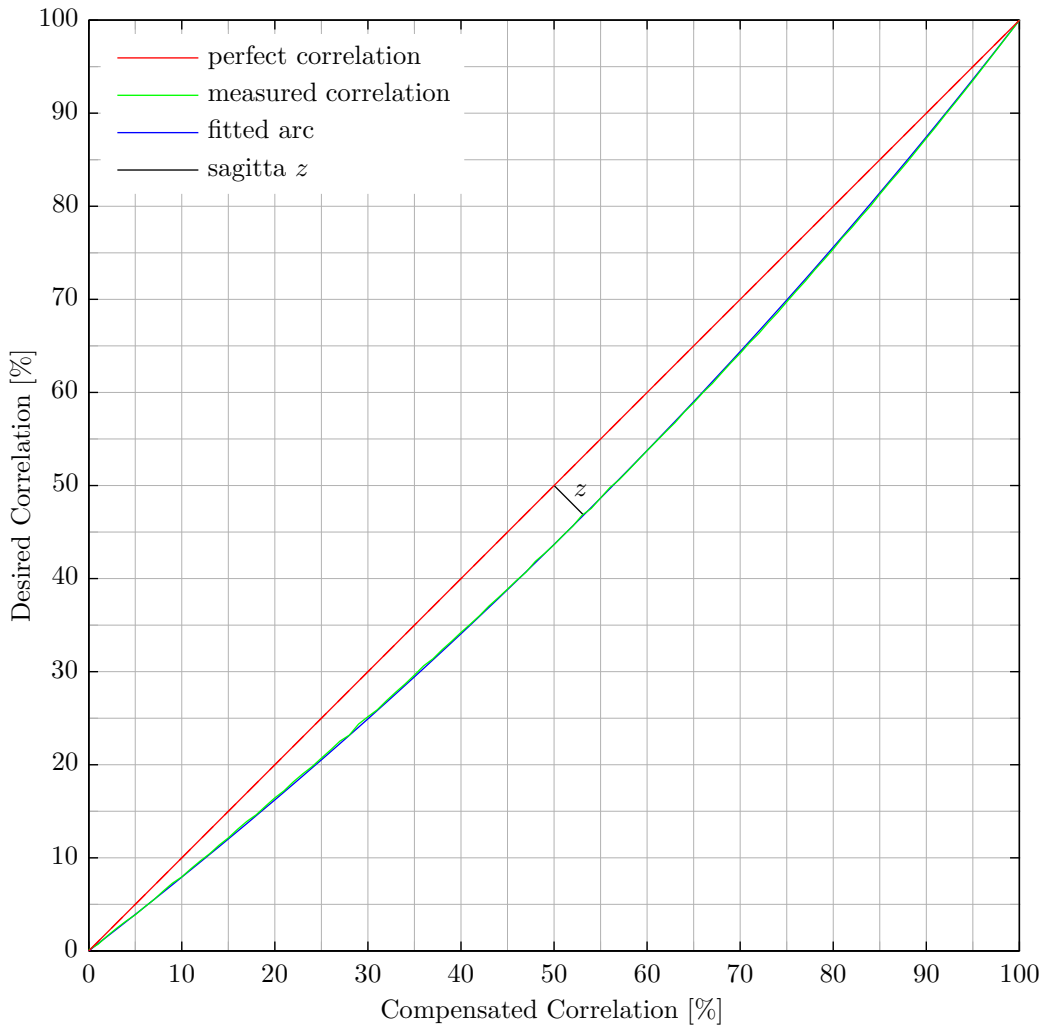


Figure 3.6: Correlation characteristics of generated beta random variables

of our generated β -distributed random variables with the same parameters. The bias can clearly be seen and is represented by the non-linearity.

We measured the bias for different parameter combinations and developed an algorithm for its compensation. The bias characteristic can be approximated by an arc with the straight line of perfect correlations as a chord. For this fit we used the least square algorithm. The length of the sagitta depends on the parameters. The sagitta is a distance perpendicular to the chord from the midpoint of this chord to the arc.

The formula of the circle is:

$$r^2 = (x - x_M)^2 + (y - y_M)^2 \quad (3.36)$$

where r is the radius, x_M and y_M are the coordinates of the center point and x and y are describing a point on the circle. Instead of this formula, we need a different function for our fitting computation. We used following functional equation:

$$y = y_M - \sqrt{r^2 - (x - x_M)^2}. \quad (3.37)$$

This function returns one y -coordinate corresponding to a given x -coordinate of the circle which we need for our calculation. All unknown x_M , y_M and r depend on the unknown sagitta z . The coordinates of the center can be calculated as follows

$$x_M(z) = \frac{2z^2 + 2\sqrt{2}z - 1}{4\sqrt{2}z} \quad (3.38)$$

$$y_M(z) = \frac{-2z^2 + 2\sqrt{2}z + 1}{4\sqrt{2}z} \quad (3.39)$$

and the radius by

$$r(z) = \frac{2z^2 + 1}{4z}. \quad (3.40)$$

Now, we can fit an arc for each set of distribution parameters α_1 , β_1 , α_2 and β_2 with the variation of the sagitta parameter z and can find the optimal z with the method of least squares.

This method can also be applied to distributions with different shapes, but for this case the application of this method has limitations. The maximum possible correlation is limited to the difference in shape. A correlation of 100 % can only be achieved with exact equally shape parameters.

This arc fitting algorithm allows us to generate almost perfectly positive correlated β -distributed random variables with a specific desired correlation between 0 % and 100 % for distributions with same shape parameters.

For verification purpose, we ran the simulation for generating those random variables in combination with this algorithm. The result can be found in Fig. 3.7. The correlation values are rounded to the first decimal place after the comma. This proves that our algorithm works quite well.

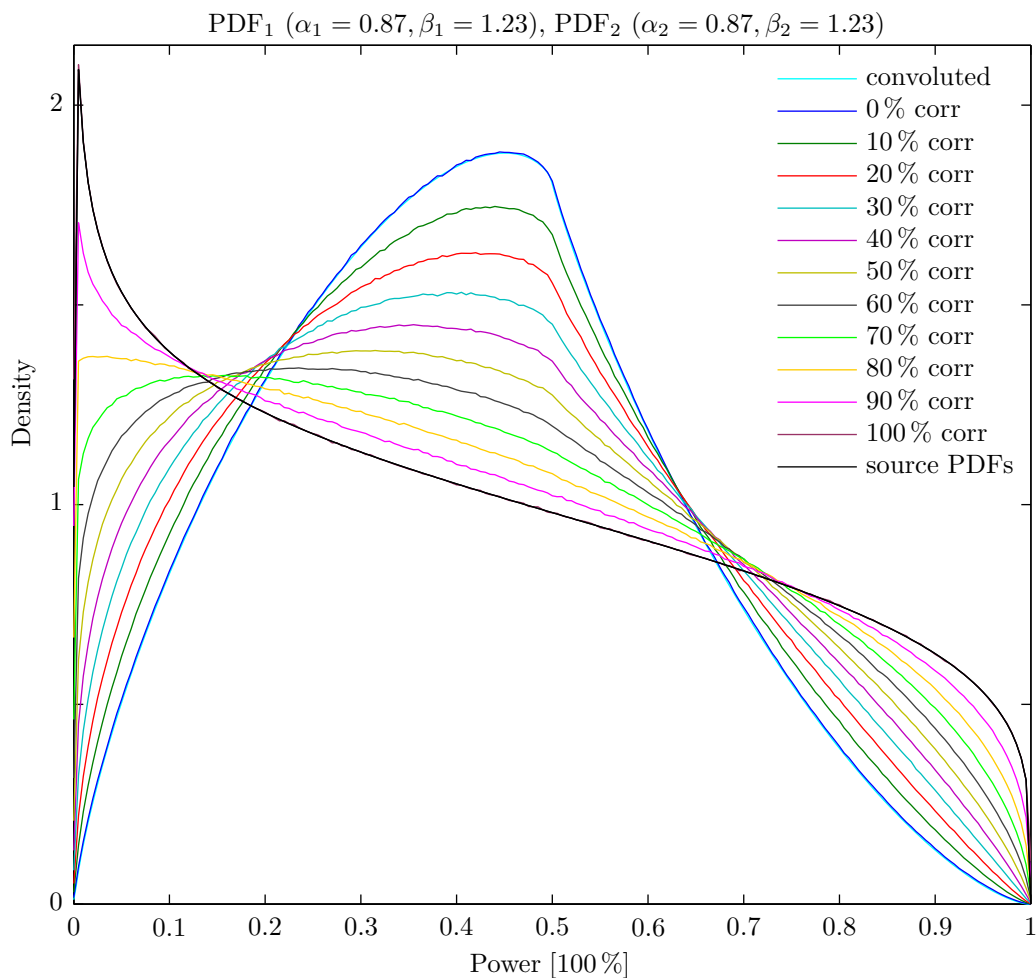


Figure 3.7: Perfect positive correlation and distributions with same shape

In Tab. 3.1 we show a summary and comparison of correlated random variables generated with different methods. At the end of each calculation run the values are slightly different. Therefore, all values in the table have exemplary character and shall not be taken as they are. The original method introduced by Magnussen is listed as method 1 in this table. Our adapted method as described in section 3.2 is referenced as method 2 and the enhancement of this method as presented in section 3.4 is referred to as method 3.

We generated random variables by using these three methods for a cor-

Desired Values	Generated Correlation with			Calculated Bias for		
	Method 1	Method 2	Method 3	Method 1	Method 2	Method 3
0	-0.07	-0.06	-0.01	————	————	————
5	2.59	4.08	5.12	48.20 %	18.40 %	2.40 %
10	4.88	8.04	10.04	51.20 %	19.60 %	0.40 %
15	7.44	12.03	15.08	50.40 %	19.80 %	0.53 %
20	9.98	16.33	20.10	50.10 %	18.35 %	0.50 %
25	12.43	20.72	25.17	50.28 %	17.12 %	0.68 %
30	15.03	25.16	30.20	49.90 %	16.13 %	0.67 %
35	17.70	29.64	35.12	49.43 %	15.31 %	0.34 %
40	20.32	34.11	39.97	49.20 %	14.73 %	0.08 %
45	22.99	38.88	44.99	48.91 %	13.60 %	0.02 %
50	25.68	43.52	50.00	48.64 %	12.96 %	0.00 %
55	28.42	48.62	54.95	48.33 %	11.60 %	0.09 %
60	31.27	53.67	59.88	47.88 %	10.55 %	0.20 %
65	34.08	58.86	64.78	47.57 %	9.45 %	0.34 %
70	36.93	64.29	69.82	47.24 %	8.16 %	0.26 %
75	39.92	69.74	74.76	46.77 %	7.01 %	0.32 %
80	42.72	75.41	79.77	46.60 %	5.74 %	0.29 %
85	45.67	81.21	84.83	46.27 %	4.46 %	0.20 %
90	48.76	87.25	89.86	45.82 %	3.06 %	0.16 %
95	51.80	93.52	94.95	45.47 %	1.56 %	0.05 %
100	55.08	100.00	100.00	44.92 %	0.00 %	0.00 %

Table 3.1: Correlation of random variables generated by different methods

relation range from 0 % to 100 % in 5 % steps. Afterwards, we measured the achieved correlations and compared them with the desired ones. The correlation results achieved by these three different methods were also compared with each other.

The values of the achieved correlations were rounded to the third decimal place. In the table we can easily compare the improvement from one method to the other. The bias is also calculated in percent for all three methods and

also rounded at the third decimal place. The values for zero correlation are marginal they are in such a tiny neighborhood around zero and they can be negative or positive as well. However, this does not represent any correlation at all.

These results illustrate the enhancements of our method of adaptation and linearity error compensation very well. We are now able to generate sets of β -distributed random variables with a correlation as close as possible to the desired one.

Going straight forward, we extended this compensation method to allow a perfect correlation for distributions with different shapes and positive correlation, as well. In Fig. 3.8 we show a correlation chart that is equivalent to the one represented in Fig. 3.6. For this chart, we used a shape combi-

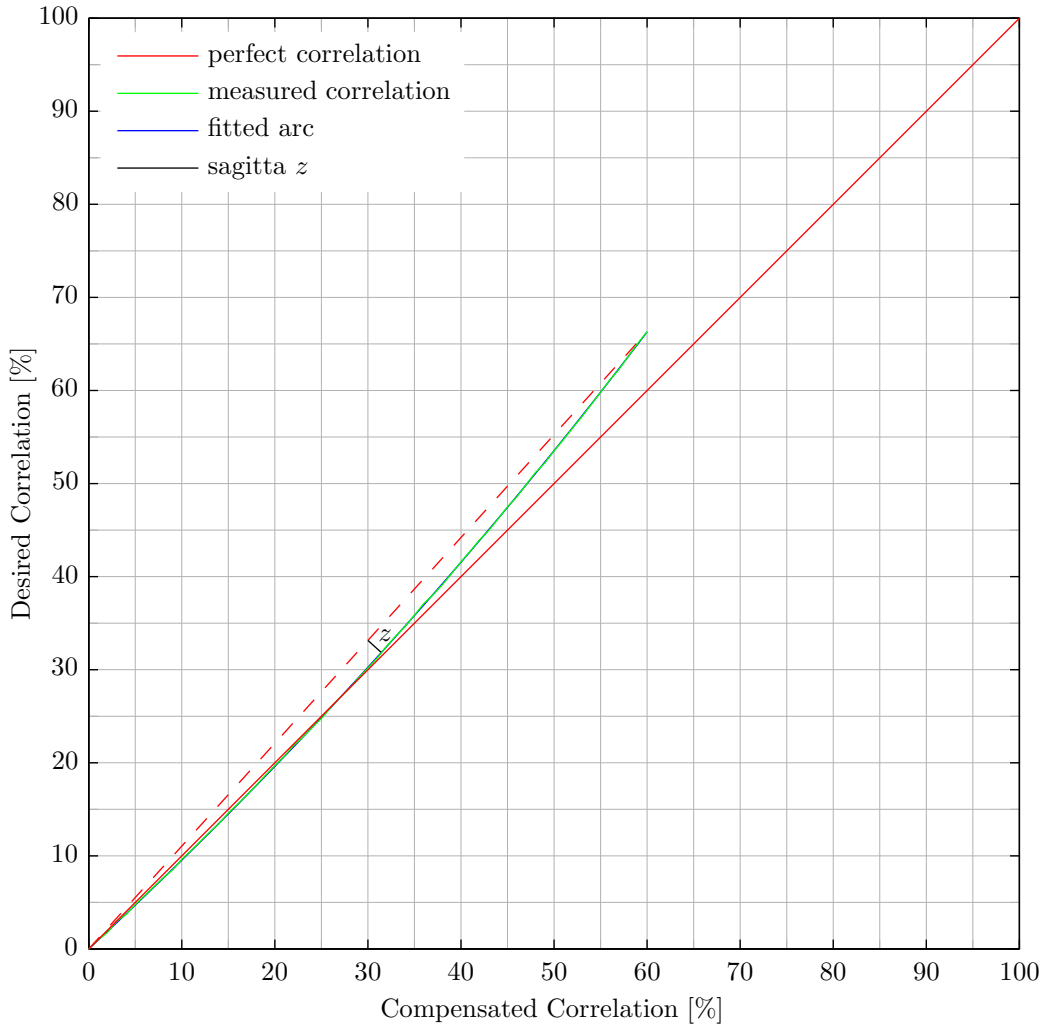


Figure 3.8: Correlation characteristics for beta variables with different shapes

nation with the following parameters: $\alpha_1 = 0.76$, $\beta_1 = 1.25$ and $\alpha_2 = 0.46$, $\beta_2 = 0.99$. For each parameter combination this chart looks different. The upper endpoint of the arc depends on the maximum correlation the shape combination can reach. The correlation characteristic is scaled down and rotated at base point $(0, 0)$. The new characteristic not only has the linearity error, it also has a pitch error.

The final arc is fitted again with the least square algorithm. The equations for calculation the new center point and the radius were adjusted. The new functions have more parameters than just z . They are also depend on the coordinates of the upper endpoint. These coordinates can be directly obtained from the correlation computation.

The value y_c is the maximum value of the achievable correlation and the value x_c can be calculated in accordance with the step width and the count of steps of the correlation computation.

$$x_c = \frac{\text{count of steps} - 1}{\text{step width}}. \quad (3.41)$$

Thus, the coordinates of the center point can be calculated as follows:

$$x_M(z, x_c, y_c) = \frac{1}{2} \left(x_c - \left(\frac{1}{2z} - \frac{z}{\sqrt{x_c^2 + y_c^2}} \right) y_c \right) \quad (3.42)$$

$$y_M(z, x_c, y_c) = \frac{1}{2} \left(\left(\frac{1}{2z} - \frac{z}{\sqrt{x_c^2 + y_c^2}} \right) x_c + y_c \right) \quad (3.43)$$

and the radius as shown below:

$$r(z, x_c, y_c) = \frac{2z^2 + \sqrt{x_c^2 + y_c^2}}{4z}. \quad (3.44)$$

With this extension of the linearity error compensation, correlated random variables for different β -distributions can be generated and the target correlation can be matched as closely as possible. This method is tested only with positive correlation and shape parameters where $\beta > \alpha$.

3.5 Linear Interpolation of Two Correlated Probabilistic Density Functions

The focus of this investigation is again on positively correlated same shaped distributions. It is a fact that 0% correlation and 100% correlation are the boundaries of correlation and also in general the probabilistic density functions of 0% and the 100% correlation are also boundaries for the curves representing the probabilistic density function between them. At the intersection areas between the original distribution curve and the convoluted one, this PDF boundary statement is not applicable but for the other areas and the largest range the statement is valid. This can be seen at Fig. 3.9. The circled areas are the intersection areas.

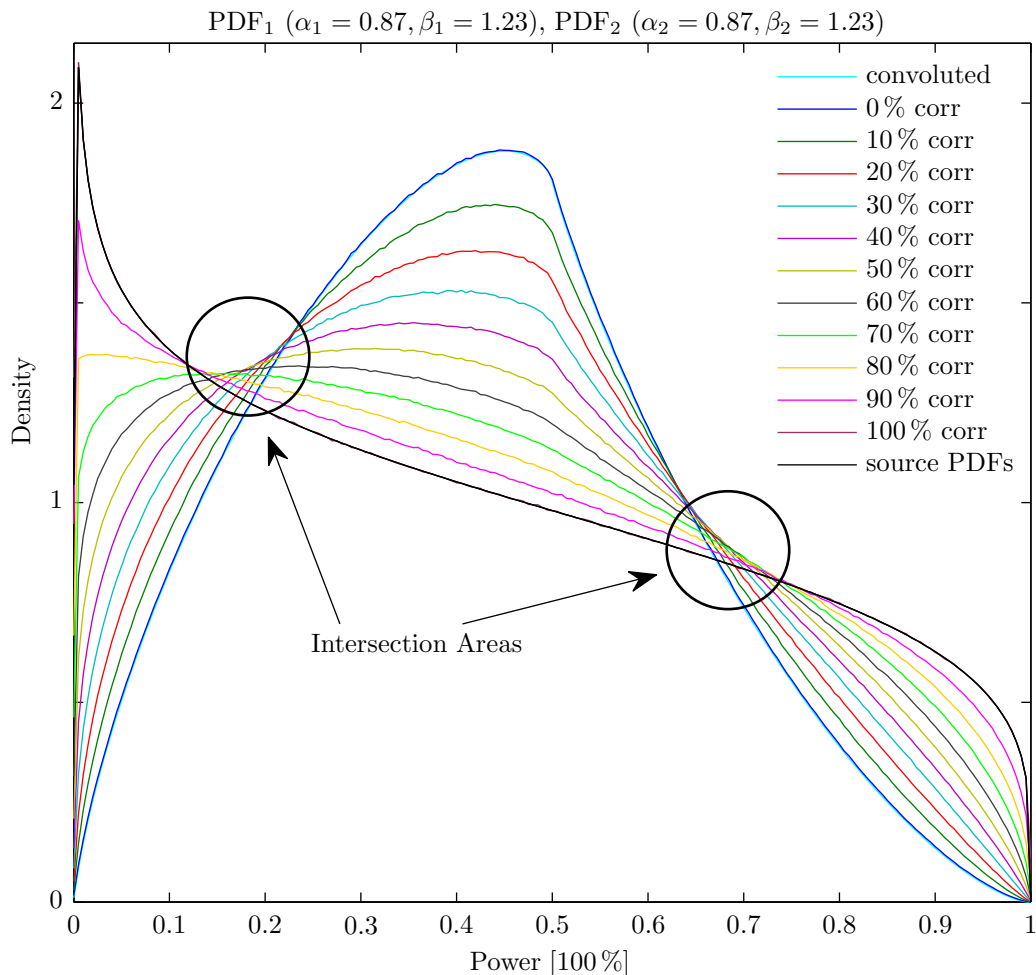


Figure 3.9: Intersection areas

Because of this fact, we started to investigate a linear interpolation of probabilistic density function between the original probabilistic density function and the one from the convolution result. We calculated probabilistic density functions for every ten percent step of correlation with respect to section 3.4. Therefore, we can compare the interpolation results with the results from our simulations. The 0% correlation curve is equal to the calculation result of the convolution computation. The 100% correlation curve is the probability density function of the given β -distribution with parameters $\alpha_1 = \alpha_2 = 0.87$ and $\beta_1 = \beta_2 = 1.23$.

A set of density functions representing the full range of positive correlation can be seen in Fig. 3.10. It is clear that in this case the intersection areas are shrunken to the actual intersection points of the two main curves 0% and 100% correlation. All interpolated graphs are intersecting at these points.

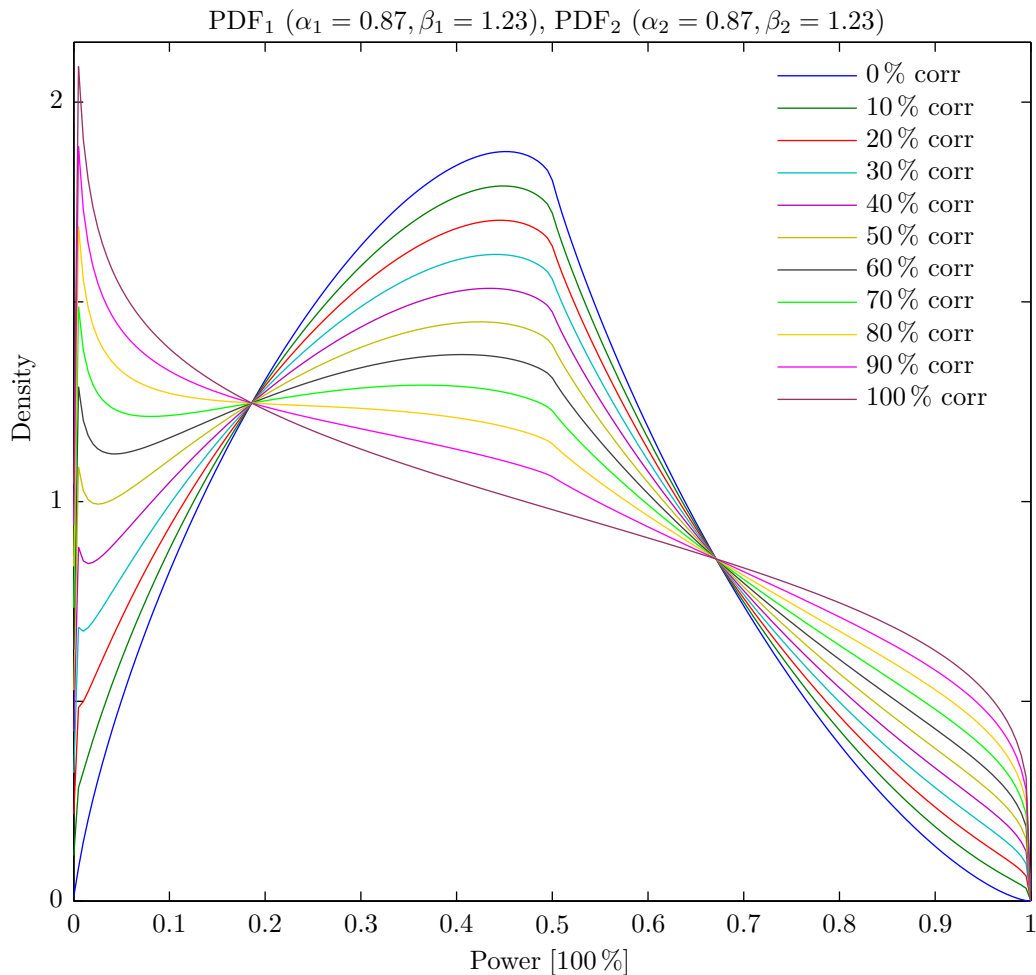


Figure 3.10: Linear interpolation result

In Fig. 3.11 we overlay the original diagram as shown in Fig. 3.9 and the interpolation result from Fig. 3.10 to show the similarities and differences between time series calculation and interpolation result. We can see there are more parameters needed to achieve a better approximation in further research. In general the time series calculation is not really linearly distributed. Especially at zero, there are huge deviations. Also at one, there are different angles making a larger deviation. The differences are highest in the middle at 50% correlation. This should be part of further investigations.

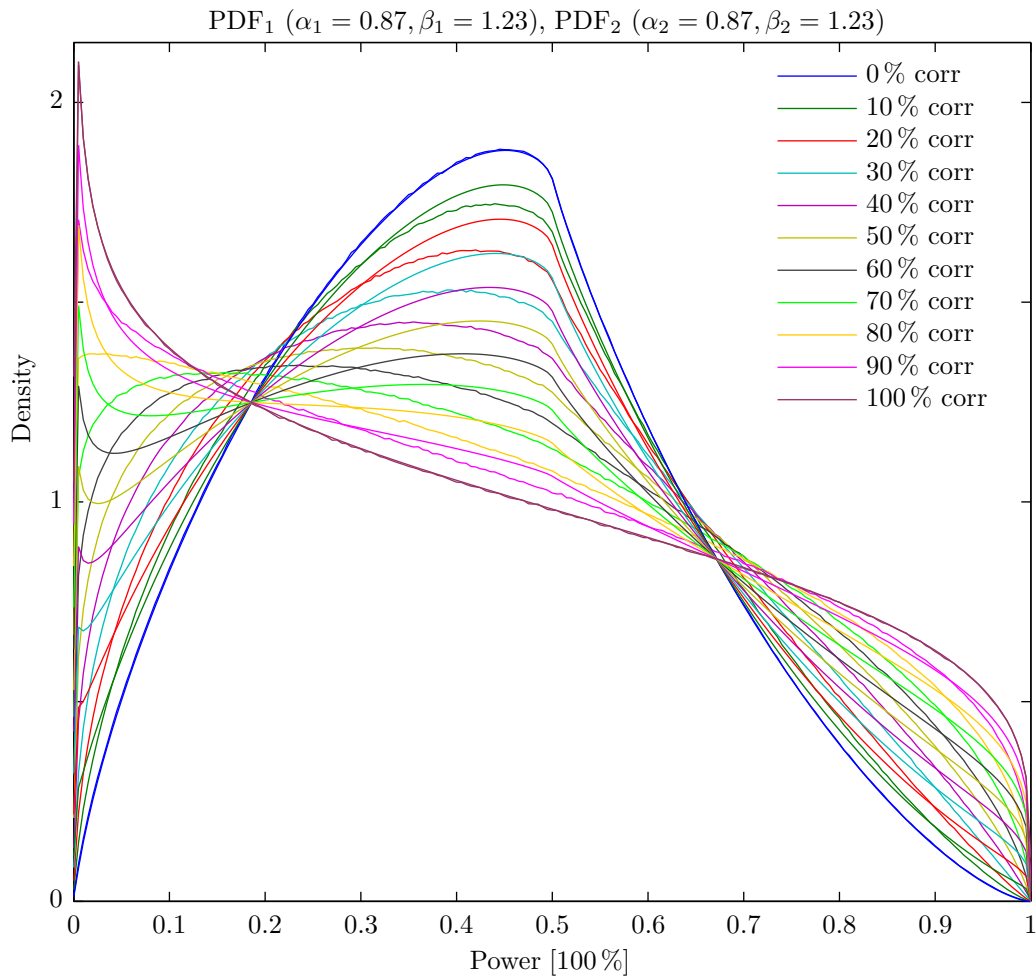


Figure 3.11: Simulation result with overlaid linear interpolation result

Chapter 4

Probabilistic Power Flow for Wind

4.1 Monte Carlo Simulation

We decided to use the Monte Carlo Simulation method for our research. This is the only method where we can compute and simulate all required scenarios without numerous restrictions or unwanted approximations.

4.1.1 Model

We used an effective model with three buses and three branches to satisfy all our requirements as shown in Fig. 4.1. The model consists of two wind power injections W_1 and W_2 , one load L , and the slack S . The slack is required to counterbalance any differences between the sum of the power of the wind generation and the load.

To define our test case, we specify important parameters for our model. The parameters we decided to use for all lines to describe this model are

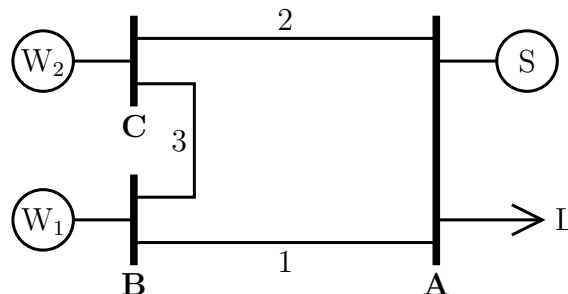


Figure 4.1: Model with 3 buses and 3 branches and 2 wind power injections

shown in Tab. 4.1. The series reactance X_l is represented in per unit and the transfer limits are in absolute values.

Line Number	Start bus	Final bus	X_l	Transfer limit
1	A	B	0.50	135 MW
2	A	C	0.33	180 MW
3	B	C	0.45	100 MW

Table 4.1: Definition of line parameters for 3 bus and 3 branch test system

For the DC load flow simulation we extended the model to four buses and four branches as documented in Fig. 4.2. We split the mutual bus A into separate buses for the slack and the load. This was done to simplify the process for the DC load flow algorithm for which each injection, load, or slack requires its own bus. We placed the slack at a separated bus and connected it with the load bus by an idealized line. From the electrical point of view, this alteration achieves the same result than directly connecting the slack with the load bus.

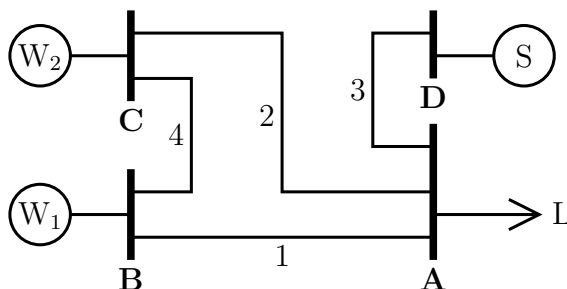


Figure 4.2: DC load flow model with 4 buses and 4 branches

The distribution of this line is not considered significant for our simulations, because it only connects the slack and transfers the required power to compensate the imbalance. Therefore, it is neither relevant nor an interesting power flow over this line. All the injected wind power flows through branches one and two to bus A, partially via the line between bus B and C.

The modified model needs a changed table of parameters. For that reason, the table above was extended by a row for the new ideal line. The line numbering was re-arranged with respect to this additional branch. The new listing with respect to Fig. 4.2 can be found in Tab. 4.2.

Line Number	Start bus	Final bus	X_l	Transfer limit
1	A	B	0.50	135 MW
2	A	C	0.33	180 MW
3	A	D	ideal connection line	
4	B	C	0.45	100 MW

Table 4.2: Definition of line parameters for 4 bus and 4 branch test system

4.1.2 Input and Output

Our method uses probability density functions as input for every power injection or node of load. For power injection we selected β -distributions as type of density functions. The distributions used for our work are fully described by their parameters. The distribution parameters are the most effective and best inputs for our method.

In addition to the statistical distribution of the power generation, we also need the maximum power output for each power plant. With this information, the density functions can be scaled correctly. Thus, all distributions are completely determined.

Another important input variable is the correlation. It can be defined as a vector representing a range of different correlation levels. We simulate a full scenario for each correlation factor of this vector and summarize the results in one chart to simplify comparison.

For the distribution of the load we looked at real data from the *Bonneville Power Administration* [3]. The data for each year can easily be estimated by a Weibull distribution [99]. The standard Weibull distribution is defined as

$$f(x, \alpha, \lambda) = \frac{\alpha}{\lambda} \left(\frac{x}{\lambda}\right)^{\alpha-1} e^{-\left(\frac{x}{\lambda}\right)^\alpha} \quad (4.1)$$

We used the data of the year 2010 [107] to compute the parameters α and λ of a fitting Weibull distribution for the load profile by a least square algorithm.

The actual power range 4230 MW-9810 MW was scaled down by a factor of ten, shifted to the origin, and fitted to a Weibull distribution between zero and five to satisfy our needs (see Fig. 4.3 for details). Loads below 423 MW do not exist in this case. These considerations for the load distribution have been used for all of our simulations.

There are a number of additional, rather important parameters to consider in our simulations. The most important ones are the discretization resolution of probability distribution, and the sample count of random variable

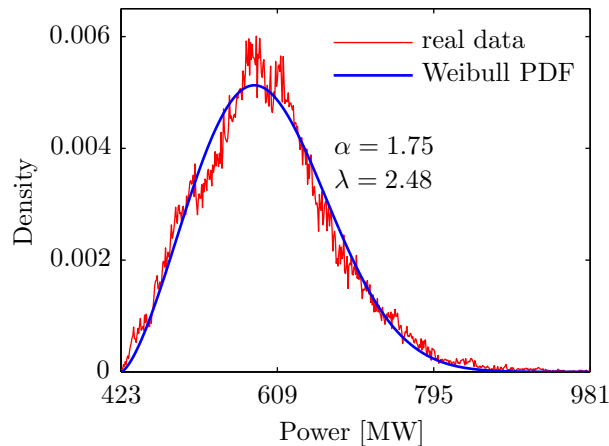


Figure 4.3: Load profile

generation. In addition, the line limit can also be controlled by parameters.

The parameters and the definition of the electricity grid also represent important input data in the form of a matrix. It includes the hierarchical structure that defines which nodes are interconnected with which line. The admittance and the function of the node, like injections, load, or slack bus, are also included. In addition, an IEEE Common Data Format¹ [108, 109] file can also be imported and the data stored in this input matrix.

The outputs of our simulations are probability distributions of the load for each line with respect to the particular correlation factors. Basically, it represents a discretized distribution model. A probability density function is similar to a histogram, but for a density function the area below the curve is normalized to one.

4.1.3 Method

After the random variables are generated as described in section 3, they are applied to our simulations. In *MATLAB*, we programmed the DC load flow functions ourselves, and compared the results with the ones from *NEPLAN by BCP Switzerland* for different scenarios to validate the correctness of our code. We also programmed the routines for the implementation of the power transfer distribution factor.

As previously described, we created an input matrix where the parametrical and hierarchical structure of the test grid was defined. This matrix is

¹The IEEE Common Data Format is a structured table of information especially to describe a power grid topology and technical data ranging from small up to large-scale grids defined by the IEEE

formatted like the IEEE common data format. The DC load flow calculations are based on these grid definitions. Therefore, the power flow direction is represented by the algebraic sign of the power flow result.

Electrically, a negative power flow makes no sense on any line, so we changed the result into a positive flow with additional information about flow direction. We added an arrow with a label to show the flow direction to the diagram and show a graph for each flow.

4.1.4 Scalability

The described and used model (with three buses and three branches) is not only the smallest one possible, but – and even more importantly – it is the most effective one to explain the algorithm. In addition, this algorithm does not only work with this small model, the model can be extended to a larger system with a significantly higher number of buses and branches.

The algorithm was applied to the grid topology of the IEEE 14-bus power flow test case [110], see Fig. 4.4. Only the injections and loads were adapted. The scalability of the algorithm of correlation is limited by the accuracy. The more variables are correlated to each other the lower is the accuracy of correlation.

For three correlated variables, the algorithm works quite well. However, for a larger number of variables correlation can be a limiting factor. The shared variables have smaller values if more variables need to be correlated to each other. The smaller the values of shared variables, the higher is the inaccuracy. In Tab. 4.3 we show an example of a correlation matrix when three injection nodes A–C are correlated with each other.

	A	B	C
A	×	0.6	0.3
B	0.6	×	0.4
C	0.3	0.4	×

Table 4.3: Example correlation matrix with 3 buses

However, there is no limitation on uncorrelated groups of small clusters of correlated power generation injections and loads. So the IEEE 14-bus test case can be used with all injections and loads. Additionally, the groups and the correlation between their members must be defined.

An example of a correlation matrix for eight buses is shown in Fig. 4.4. In this matrix we show different clusters of correlated buses. Completely separated and interconnected groups of correlated nodes are included, as well as buses with just one correlation partner up to four correlated nodes.

	A	B	C	D	E	F	G	H
A	×	0.5	0.4	—	—	—	—	—
B	0.5	×	—	—	—	—	—	0.3
C	0.4	—	×	0.4	—	—	—	0.2
D	—	—	0.4	×	—	—	—	—
E	—	—	—	—	×	0.4	0.5	—
F	—	—	—	—	0.4	×	0.3	—
G	—	—	—	—	0.5	0.3	×	—
H	—	0.3	0.2	—	—	—	—	×

Table 4.4: Example correlation matrix with 8 buses

4.2 Storage

Our original simulation did not consider storage at all. In order to point to the advantage of storage, we decided to add storage at each power injection node, see Fig. 4.5. This allows not only more flexibility, but also the usage of line limits for additional simulations. These storage devices (St_1 and St_2) take care of the surplus generated by the power injections and thereby provide a meaningful alternative for the power that cannot be transferred over the lines due to limitations.

The usage of the same entirely unchanged β -distribution for power generation is now fully consistent with our test case to remain stable. With a restriction at one or more branches we could not inject the same amount of power while guaranteeing stability of the grid. Thus, with these additional storage devices at each connection node, we are able to use the uncurtailed power generated by all of our power plants and wind farms at the time when the wind occurs.

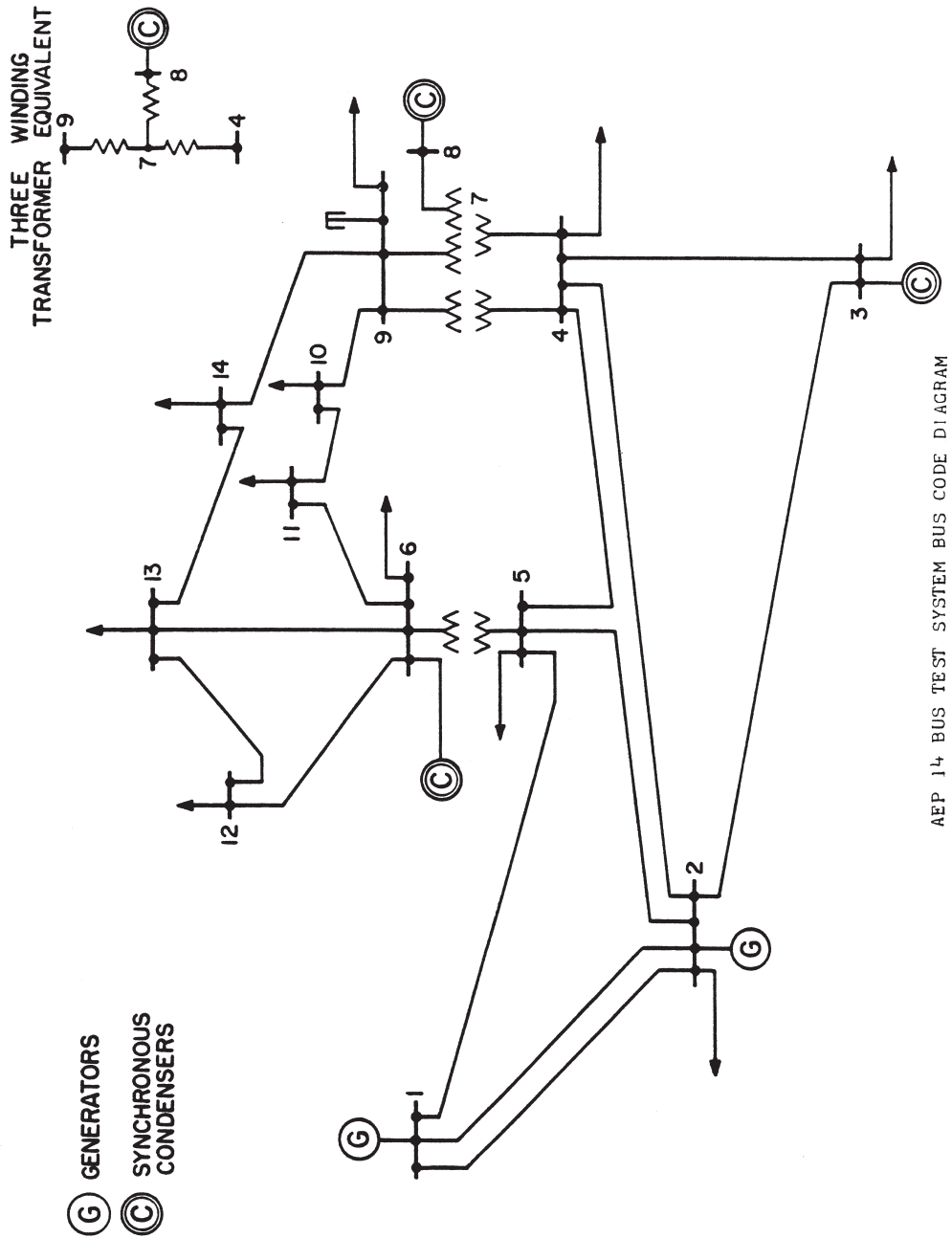


Figure 4.4: IEEE 14-bus test case

We modeled our storage as devices without conditions and limitations. This means that regardless of the power generation or transmission, the devices can release or store any additional amount of energy. We are using a theoretical model without representing any specific storage technology. In addition, we do not consider any limitations with respect to timing at charging and/or discharging the storage units.

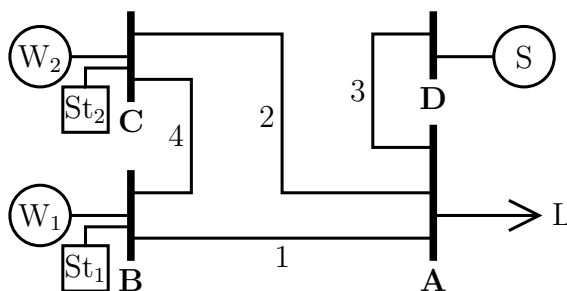


Figure 4.5: Load flow model with 4 buses, 4 branches and 2 storage devices

4.3 Line Limits

We can define a line limit of power transmission for each branch. The value of this limit represents the maximum load that the line can handle, regardless of any technical and technological reasons. It can be set to any non-negative value. In the case of line limits, we do not differentiate among different flow directions. A zero-value deactivates the line limit for the specific branch.

With a line limit we have a parameter to affect and tune the power flow in a realistic way. Normally, a connection line cannot handle the maximum power a power plant can generate. In this case the power generation will be reduced, and the curtailed power is lost. A better way would be to put the surplus into storage devices.

Chapter 5

Results & Discussion

In the following sections, we describe different simulation setups and their results. Starting with the same probability density function for all wind power injections, we changed the setup to use different density functions for each power injection. Finally, we added storage and introduced line limits. The basics for all computations are described in chapter 4. Storage and line limits are only for the section 5.3. All simulations are applied to our small model with 4 buses and 4 lines but the notations are with respect to Fig. 4.1.

5.1 Identical Wind Farms

In this section, we explain our simulations using the PDF and same power values for both of the wind power injections W_1 and W_2 as shown in Fig. 5.1. We are discussing the results and emphasize the most important facts.

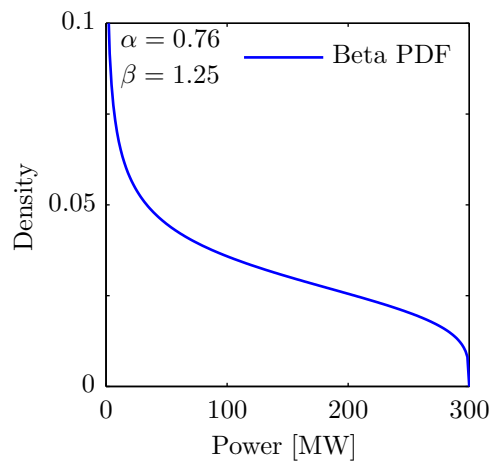


Figure 5.1: Identical Probability density function for injections W_1 and W_2

In the following three figures (Fig. 5.2 - 5.4) we show the simulation results for branch one, two and three with a positive and negative power flow. The flow direction is calculated with respect to Section 4.1.3. The black curve is the result of the convolution and the other 11 colored curves are probability density functions from our simulation calculation in ten percent steps from zero to full correlation.

The 100% curve is equal to the original probability density function of both power injections. This is not additionally shown in the following figures. On lines with only one flow direction, the direction defines the appearance. For negative flow direction, the curve is just mirrored with respect to the original one. If both directions do occur, then the PDF of power flow is a completely new one.

In the next three figures (Fig. 5.5 - 5.7) of this section, we summed up the frequency values from both flow directions to obtain the absolute amount for values of each line. This way, we can show which amount of power occurs how often with respect to all other values, regardless of the direction of flow for each line.

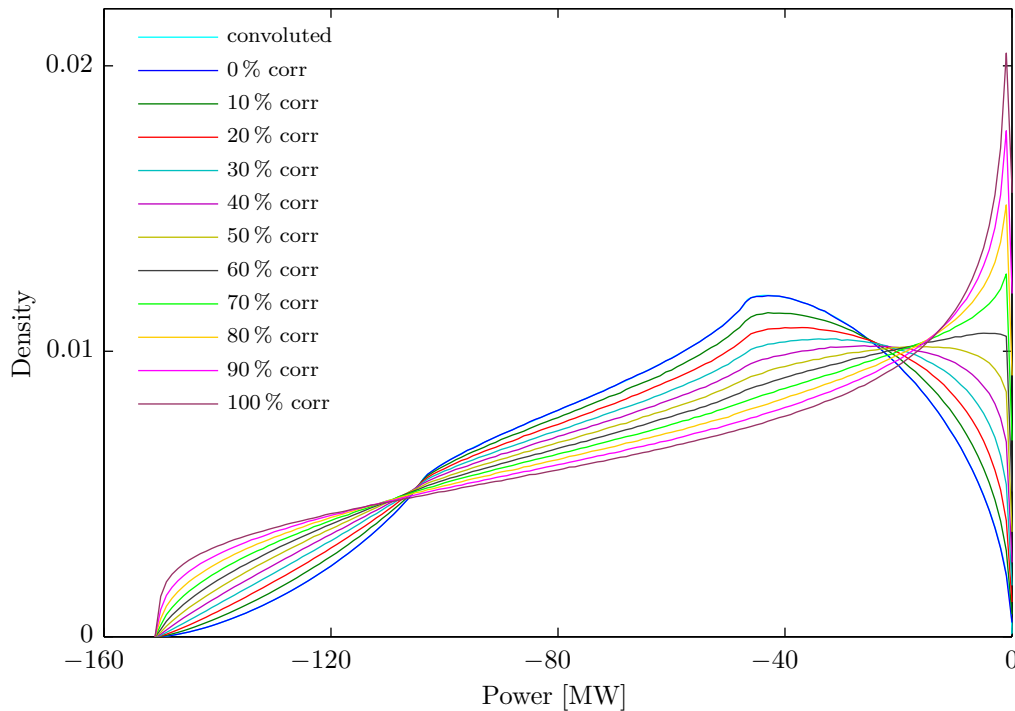


Figure 5.2: Simulation result for branch 1 including flow direction

With the setup of identical wind farms, we have the following situation: All injecting wind farms have the same parameters – only the grid parameters

(the series reactances X_l) are different and have influence on the distribution of the power flow. If the grid parameters would be symmetrically, the distribution of power flow would also be symmetrically. If the grid parameters are symmetrically and the maximum power outputs of the wind farms are different, then the difference is the determining factor for the power flow.

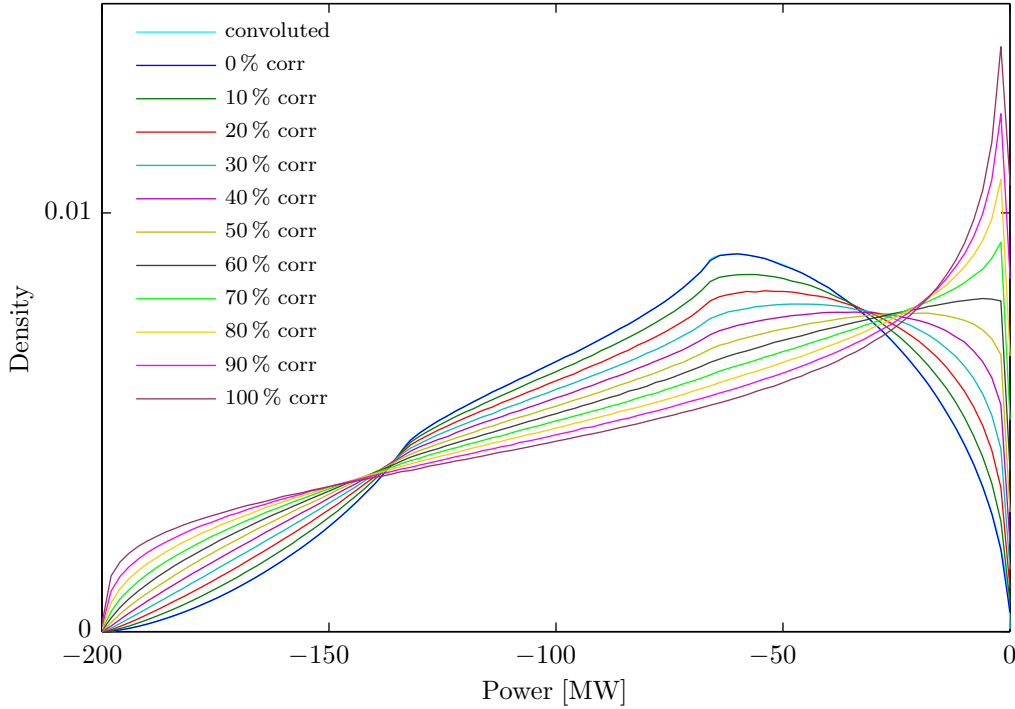


Figure 5.3: Simulation result for branch 2 including flow direction

The full range of correlation is available. On the one end of this range there is 0 % correlation (or the convolution result). At the other end we have 100 % correlation (or the original probability density function). All other correlations are between these two limits. This trend can also be seen on each and any of the following figures. The curve of the convolution calculation result and the one with the original PDF are spanning areas, where all the other graphs of the correlation range are lying inside these areas, see Fig. 5.8 - 5.10. Only at the intersection points there are some inaccuracies with respect to these areas. But besides that, we can say that the extremes of the power flow can be illustrated by the graphs of 0 % and 100 % correlation.

If we calculate the maximum of these two graphs at each point, we can find the maximum load. This approach is equally applicable to the minimum. Thus, we can find the minimum and the maximum of a line load flow without calculating anything except the original PDF and the convolution.

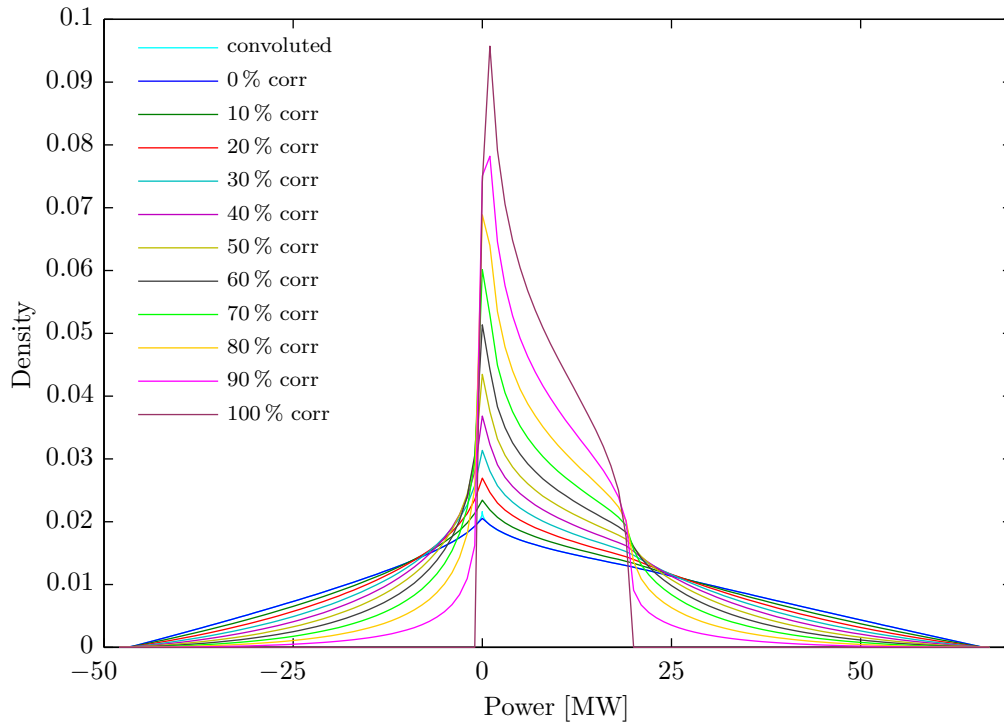


Figure 5.4: Simulation result for branch 3 including flow direction

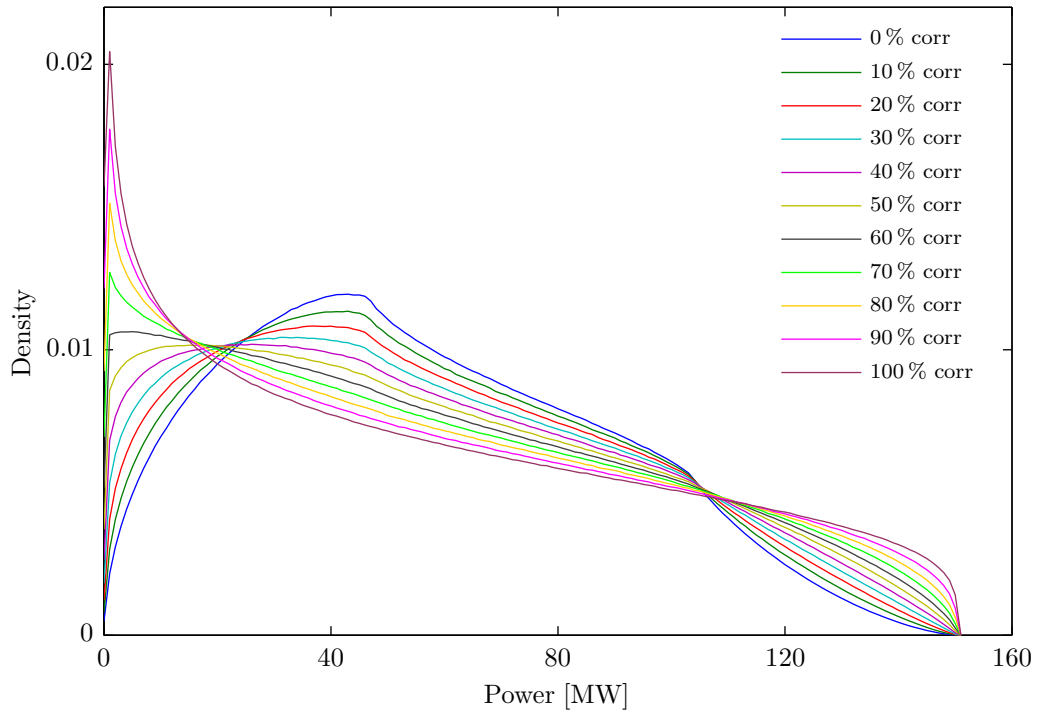


Figure 5.5: Simulation result for branch 1 with absolute values

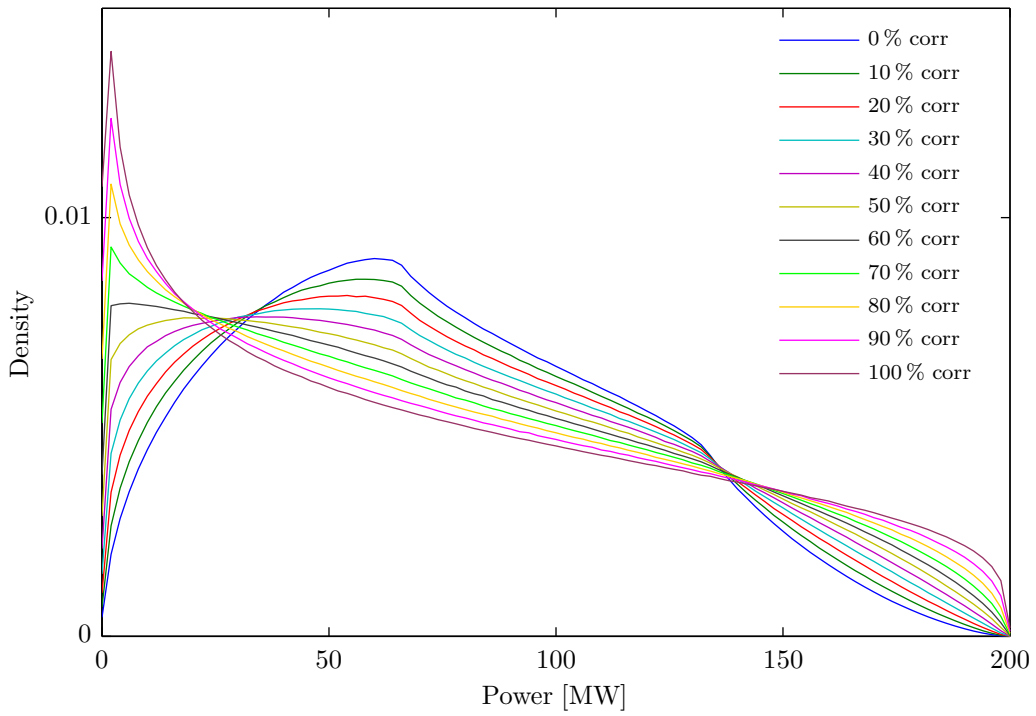


Figure 5.6: Simulation result for branch 2 with absolute values

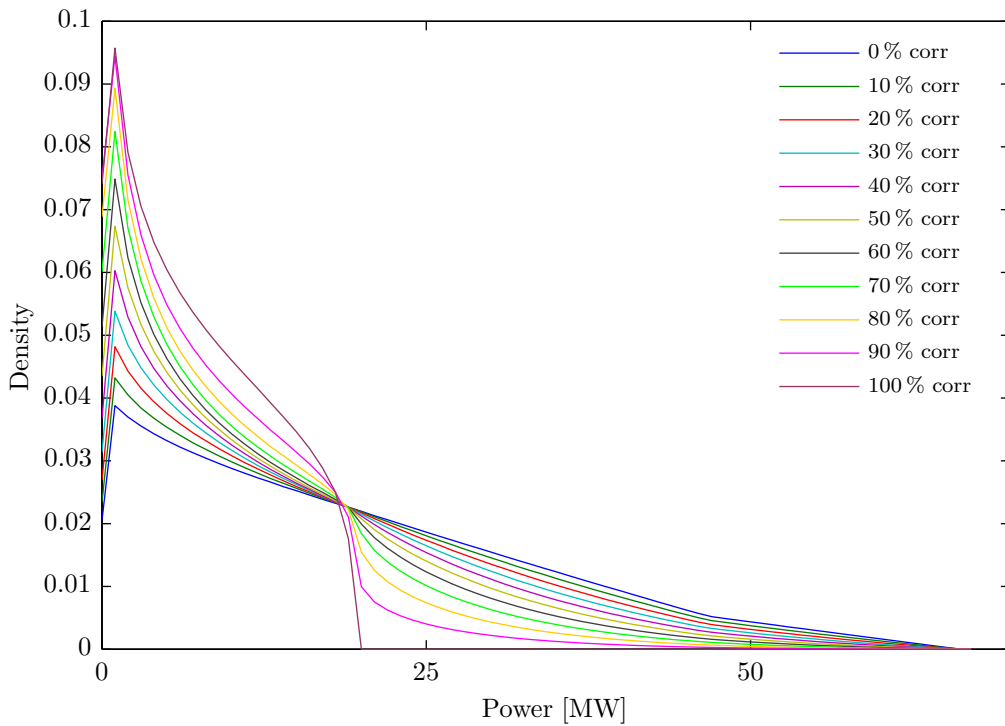


Figure 5.7: Simulation result for branch 3 with absolute values

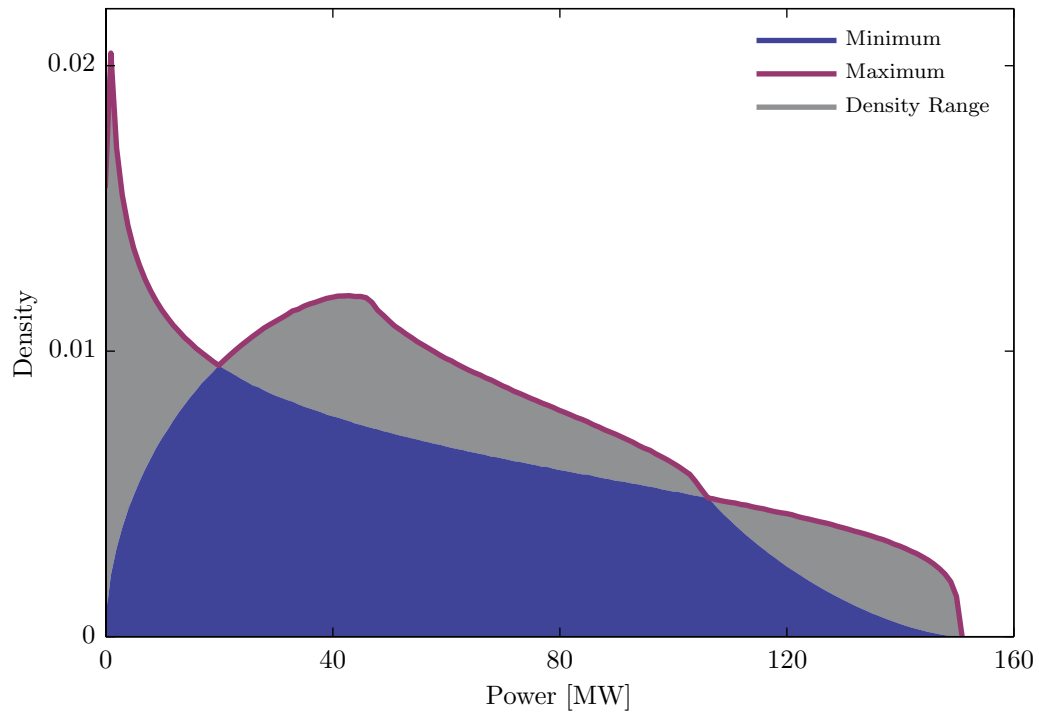


Figure 5.8: Load flow minimum and maximum of branch 1

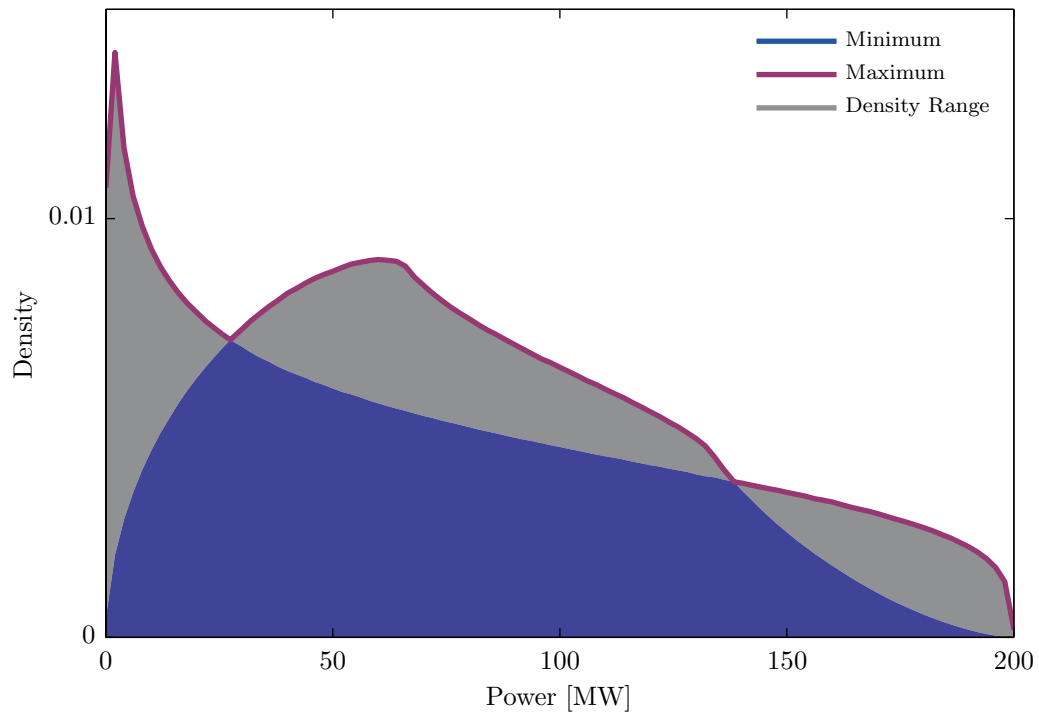


Figure 5.9: Load flow minimum and maximum of branch 2

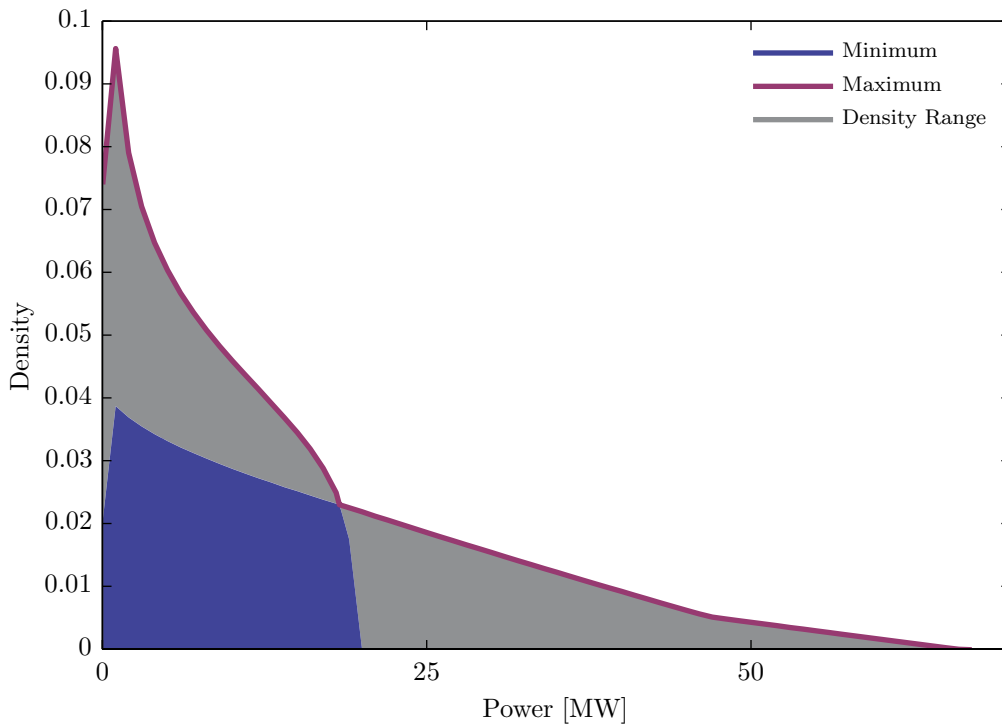


Figure 5.10: Load flow minimum and maximum of branch 3

The section with maximum values of the convolution is in the middle of the power range. That means, for less correlation it is more likely that power flow values in the mid-range occur. The probability of the occurrence of marginal values of the power range is very low.

On lines with power flow in one direction, as on branch one and two, we see following, rather interesting facts: The maximum at the areas close to the marginal values are given by the original input probability density function, the minimum by the result of the convolution. Looking from the limits into the range, we have intersection points between the curves of the original PDF and the one of the convolution, resulting in switching the minimum and the maximum with respect to the line load occurrence.

On branches with bi-directional power flow a few things change. The maximum peak is at zero. Here we can see that the maximum in the center is not given by the convolution and we cannot say, it is the original input PDF. However, we can find a scaled version of the original PDF. Again, the convolution, and in this case the scaled original PDFs are the marginal curves which bound the areas where all the correlation graphs are lying in.

With two identical input density functions, we see one to three sections at the resulting curves. The higher the correlation, the lower the count of the sections and vice versa.

5.2 Different Wind Farms

Moving straight ahead, we changed the input probability density function of wind injection W_2 at bus C, as shown in Fig. 5.11b as next step. All other

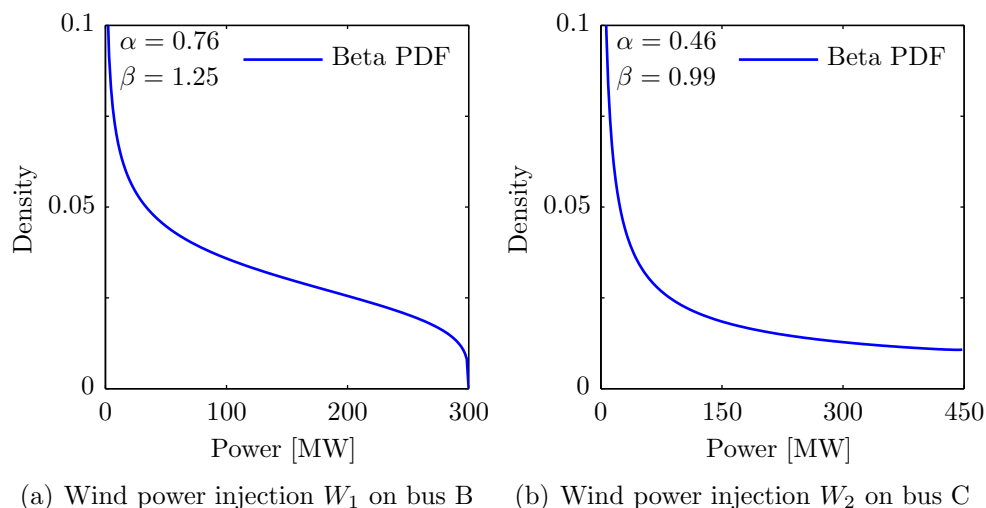


Figure 5.11: Different Probability density functions for injections W_1 and W_2

parameters remain the same.

In the following Fig. 5.12 - 5.14 we see the computation results for branch one to three and in Fig. 5.15 - 5.17 the same results converted to absolute values of the load flow of each line.

With different density functions of the injecting wind farms, it is more complicated to analyze the results. Optically, they are quite similar but there are several differences.

Firstly, we have to compute the maximum possible correlation in this combination of input probability density functions. The mix of two different PDFs is no problem for the convolution process, but the highest achievable correlation cannot be found immediately, it must be calculated. In this case, we have a maximum correlation of 60%, but we rounded to the next ten percent step. After this step, we can adapt the statement from the section of identical wind farms as follows:

The graph of the maximum correlation and the one from the convolution computation are now bordering the areas, where the other curves of the correlation range are spread within the limits, see Fig. 5.18 - 5.20. Therefore, we are required to replace the curve of 100% with the one of maximum correlation. All other conclusions can be adapted in the same manner.

The most important step is to calculate the maximum possible correlation for a given set of probability density functions. Following this exercise,

minimum and maximum of line loads can be determined.

The level of complication is significantly higher for branches with bi-directional power flows. This is much similar to the trend of identical wind farms. In the middle, the graph with the maximum correlation gives the maximum and the convolution result the minimum. Moving outwards, we reach the intersection points where the curves for maxima and minima change. After that, the graph representing the convolution gives the maximum and the curve with the maximum correlation illustrates the minimum of the load.

For lines with two flow directions, we cannot find a similar shape showing the maximum correlation as we found it in the previous section for identical wind farms. The graph representing the maximum correlation looks like a combination of both original input PDFs. The part to the right of the maximum of the curve is segmented into two sections for higher correlation and become one section for no correlation. In each section we can find an analogy to one of the original input distributions. The peak of the maximum is again at zero. We can also interpret the left side as the same mirrored PDF.

In general with two different input density functions we also detect one to three sections at each line flow graph. Every section has some similarity with the input distributions.

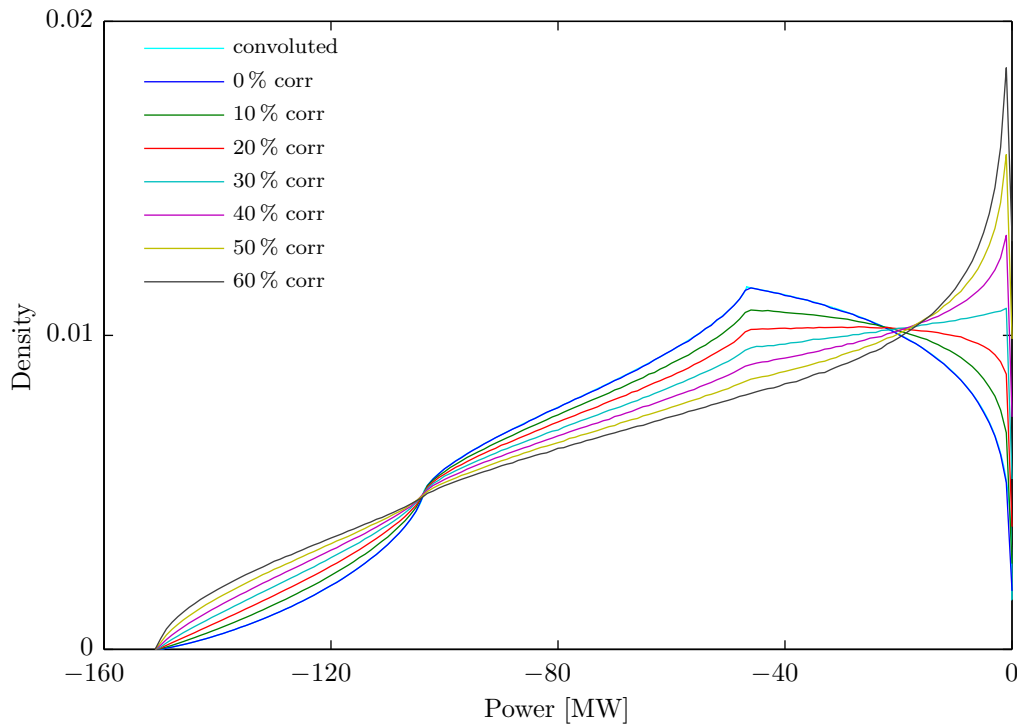


Figure 5.12: Simulation result for branch 1 with flow direction

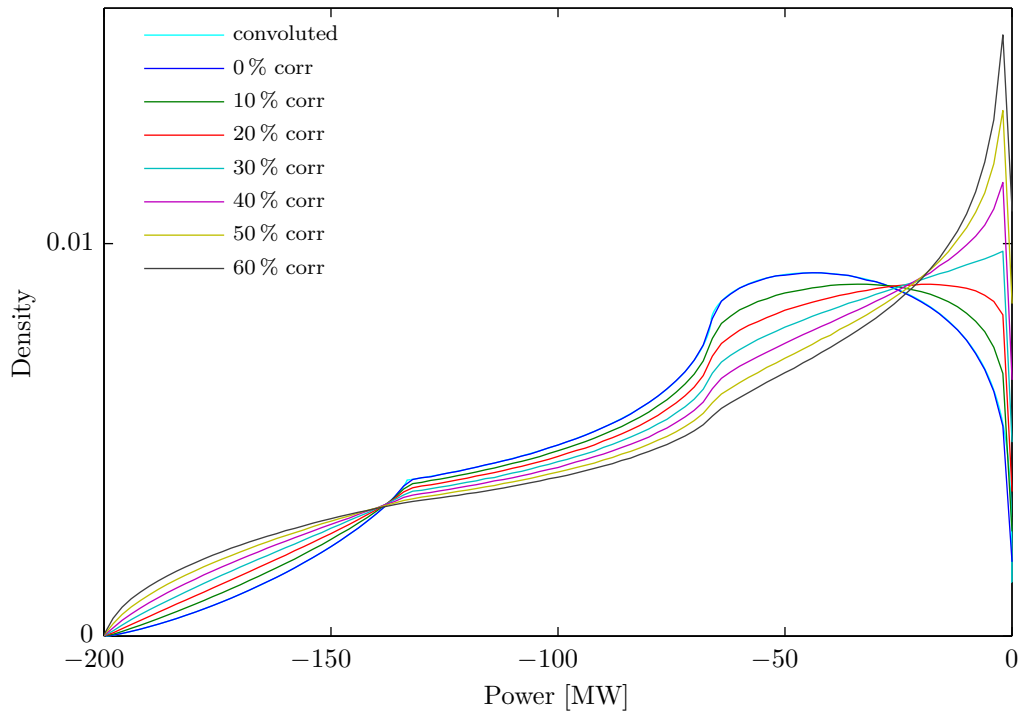


Figure 5.13: Simulation result for branch 2 with flow direction

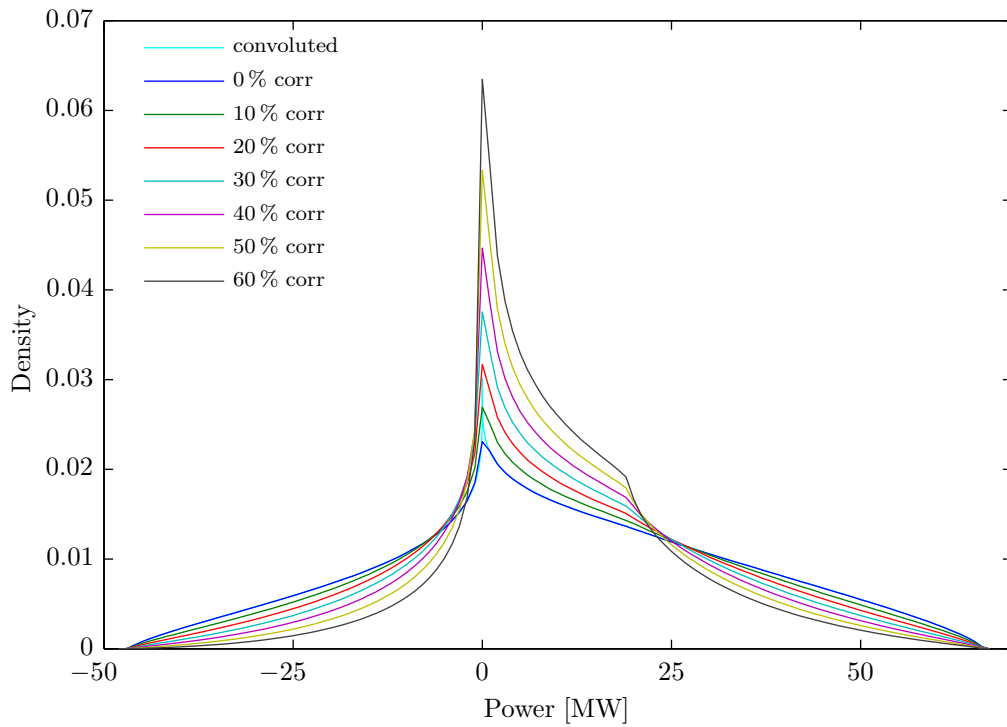


Figure 5.14: Simulation result for branch 3 with flow direction

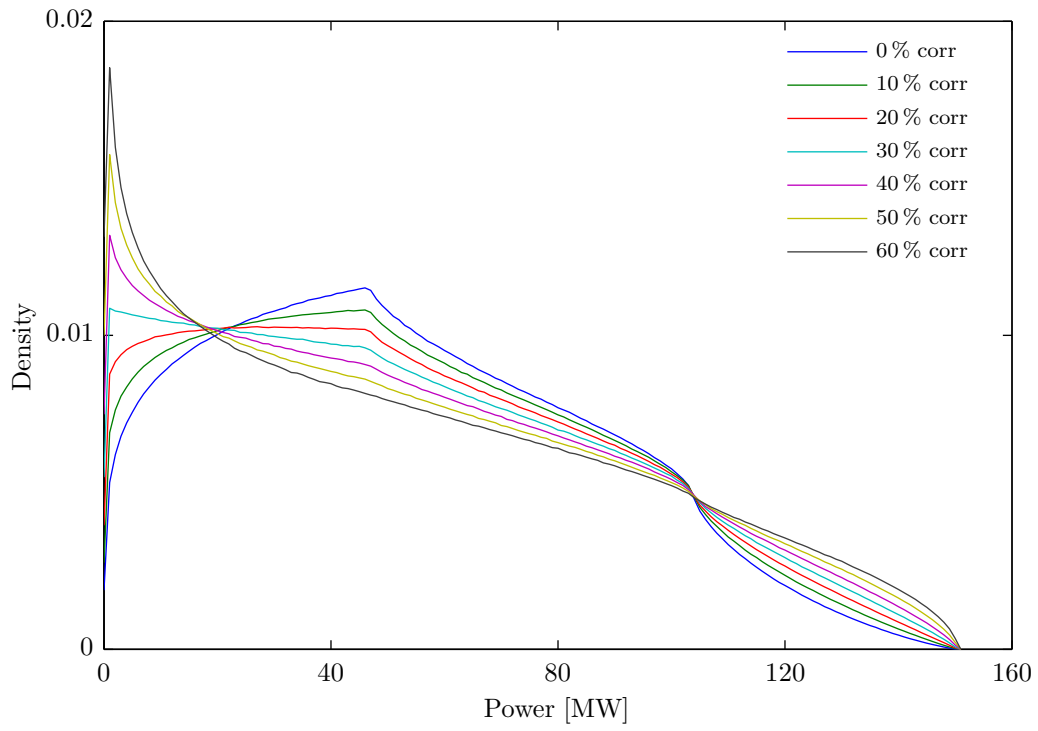


Figure 5.15: Simulation result for branch 1 with absolute values

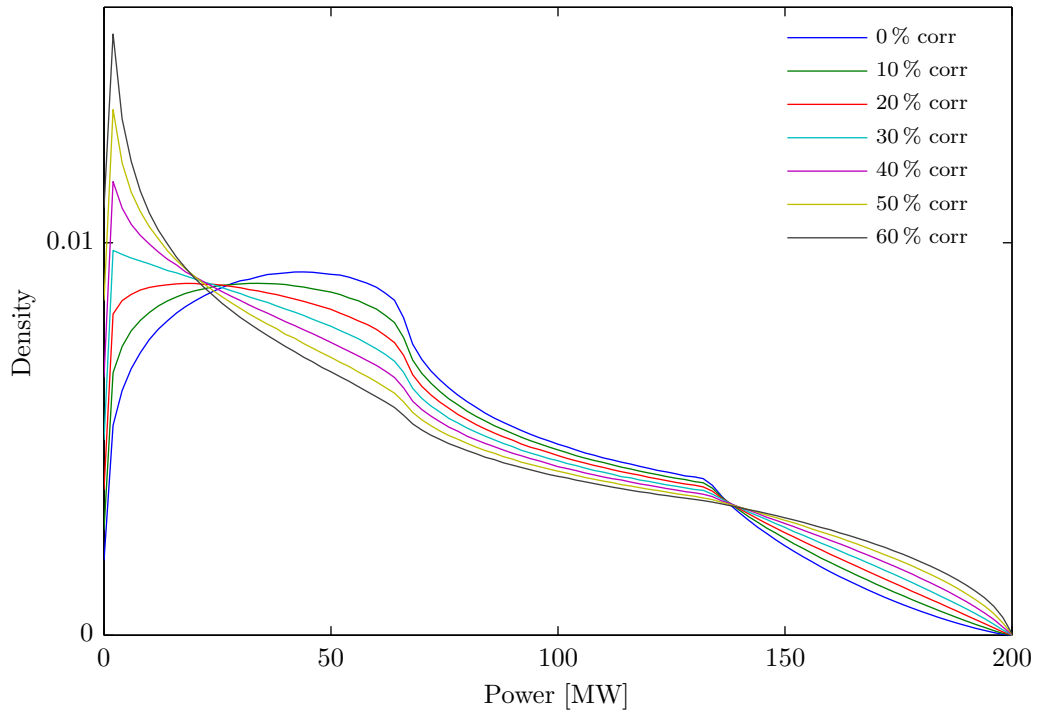


Figure 5.16: Simulation result for branch 2 with absolute values

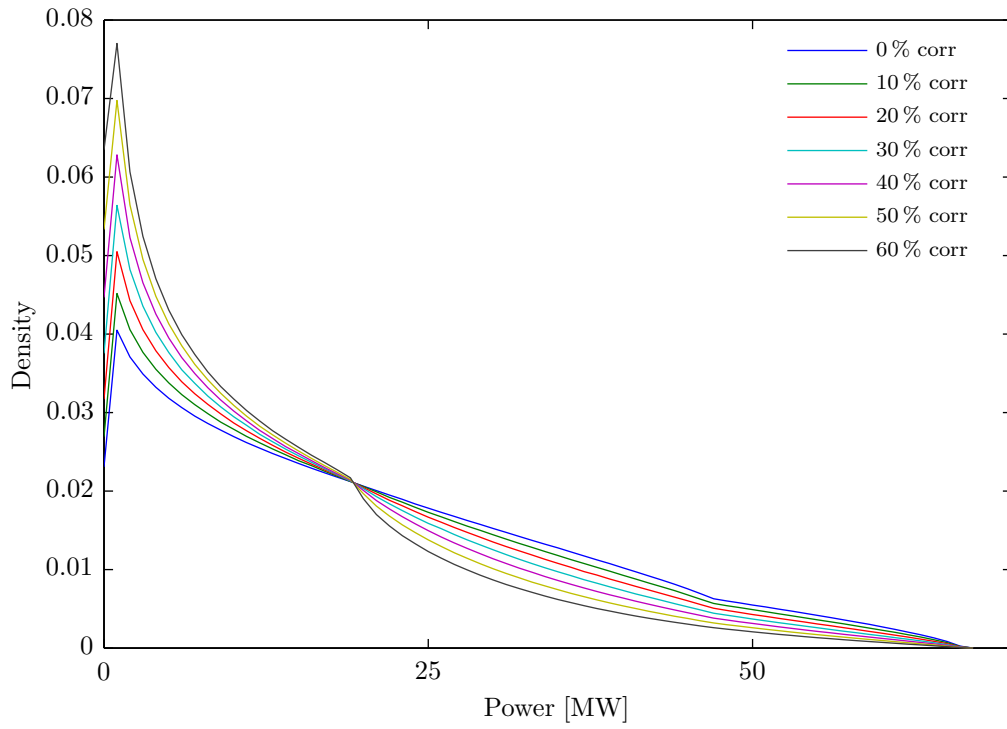


Figure 5.17: Simulation result for branch 3 with absolute values

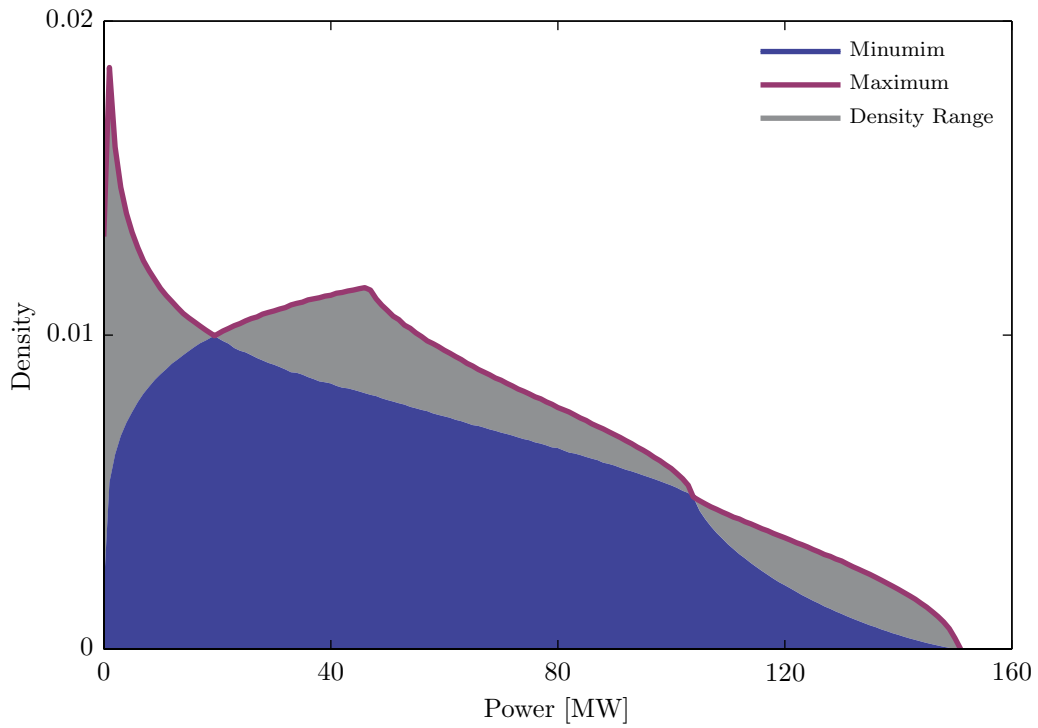


Figure 5.18: Load flow minimum and maximum of branch 1

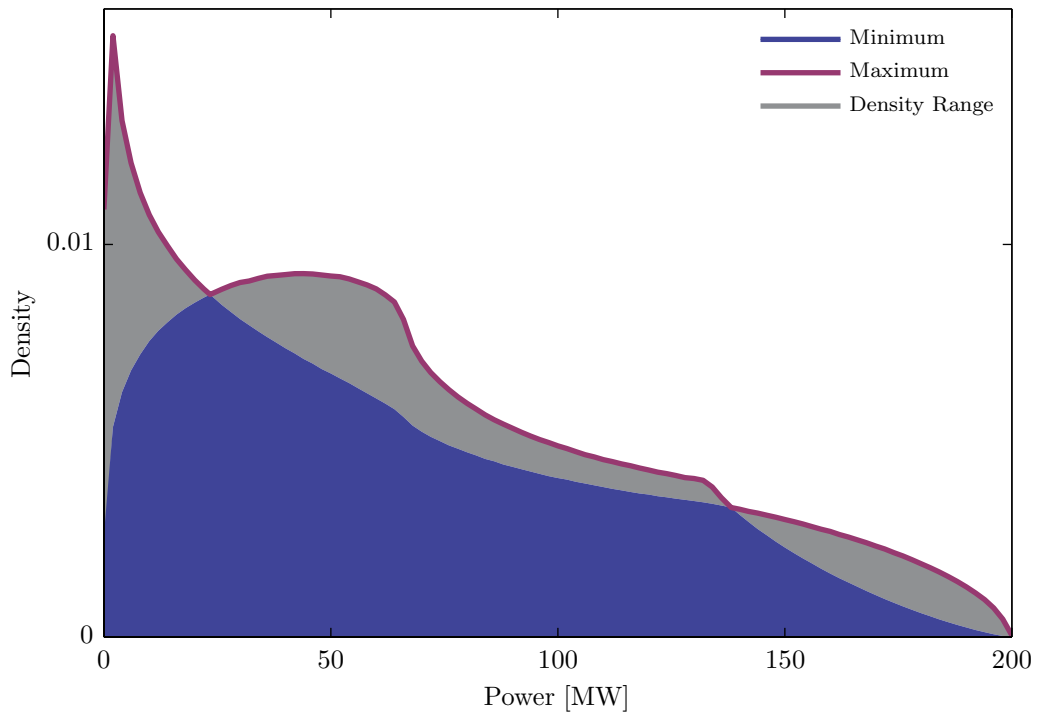


Figure 5.19: Load flow minimum and maximum of branch 2

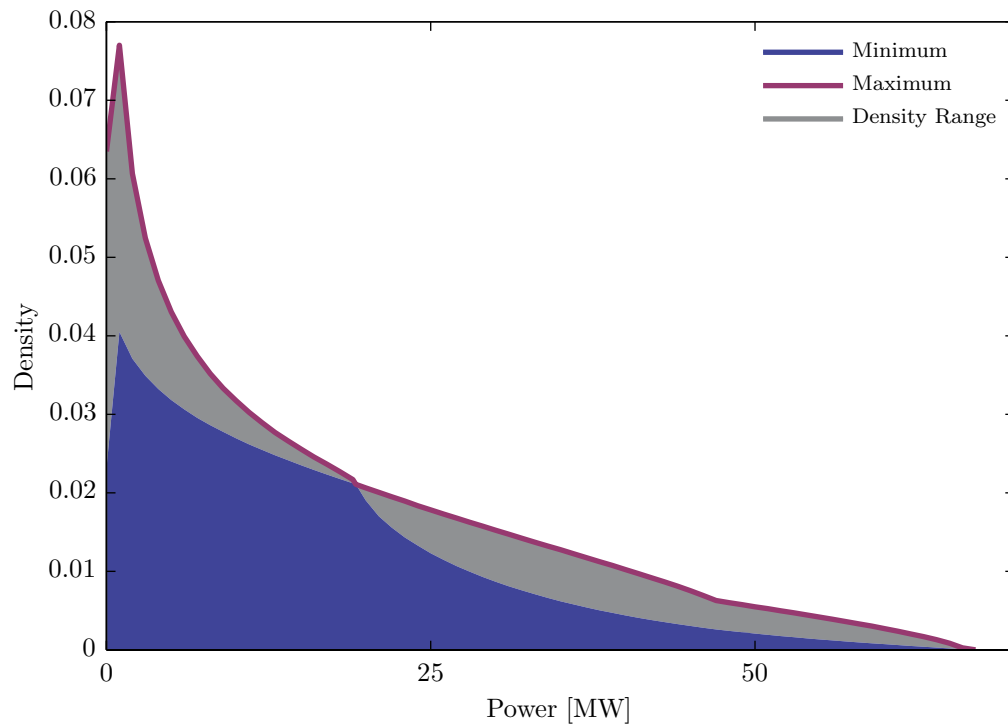


Figure 5.20: Load flow minimum and maximum of branch 3

5.3 Line Limit and Storage Extension

As additional feature of our simulations we can take line limits of the transmission lines into account. For the following simulations, we considered a line limit of 135 MW for the first and 180 MW for the second transmission line. At the injection side of each bus a storage device is located. These storage devices are being charged with the surplus of energy a line cannot handle if the value of power is higher than the limit.

The PDFs of the lines are shown in Fig. 5.21 and Fig. 5.22. We can see that there is a peak at the limit. All absolute values above this limit are cut off and so each larger power value is mapped to the value of the limit. The curve for the convolution method is not shown separately.

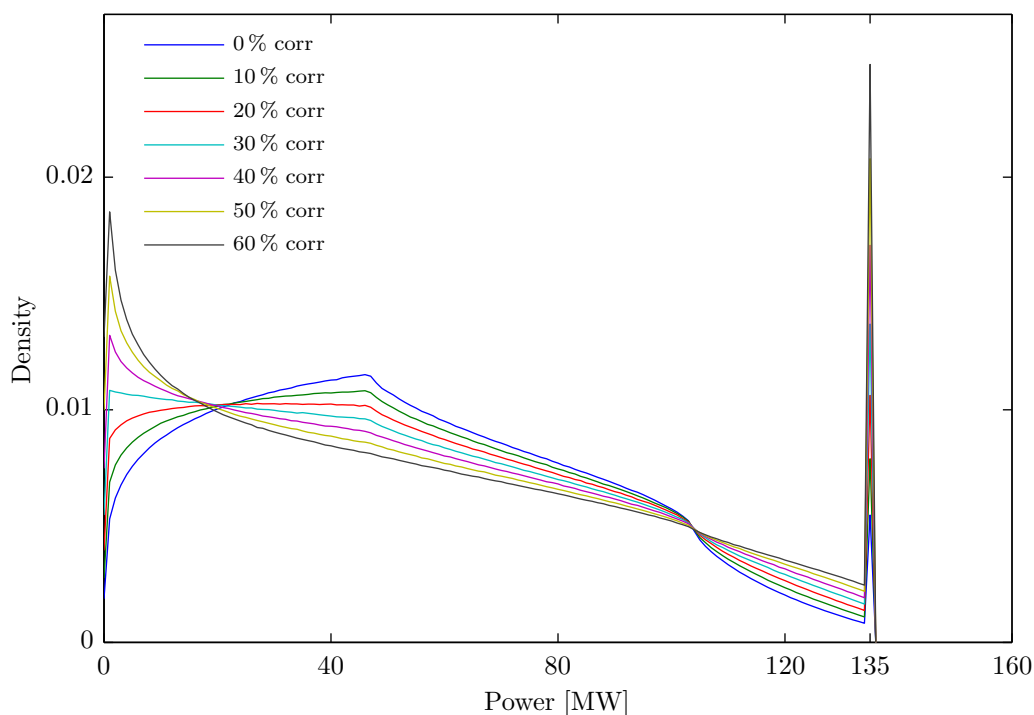


Figure 5.21: Simulation result for branch 1 with a line limit of 135 MW

In Fig. 5.23 the PDFs of the storage devices are shown. A peak at zero would represent the sum of all line flow values is below the limit and is not displayed. The presented curves are exactly the parts, which are cut-off from the lines. For the power values, the limit is subtracted from the cut off values.

With this method we can simulate the PDFs of the storage, but not of the state of charge (SoC). This is the reason why we need real data or time referenced values instead of our generated random variable series.

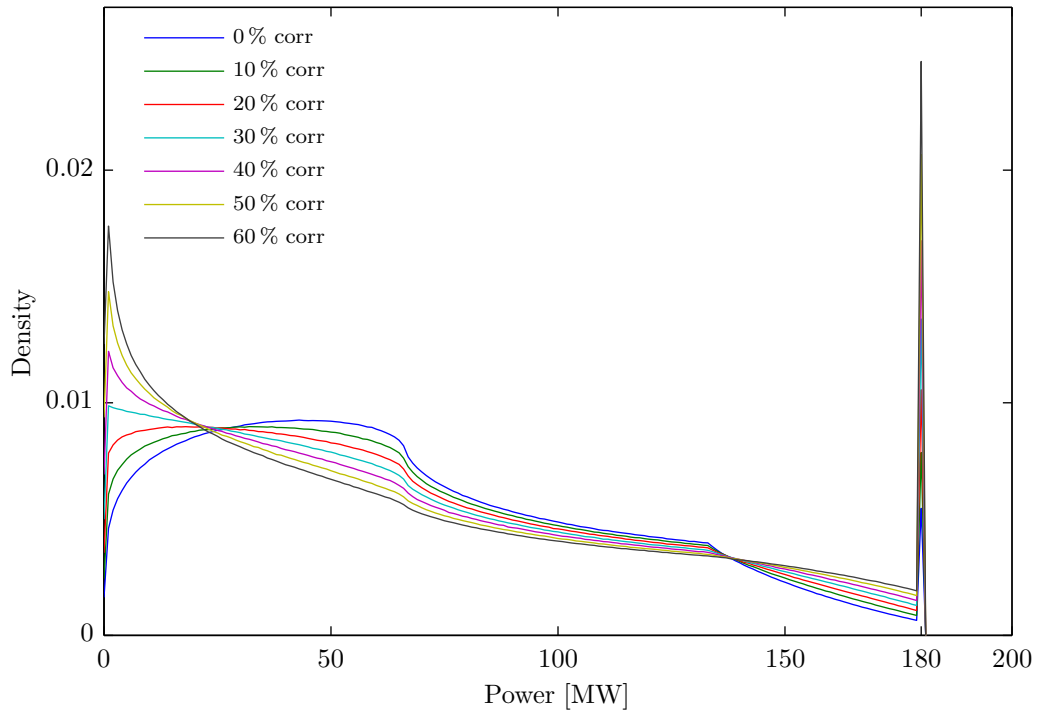
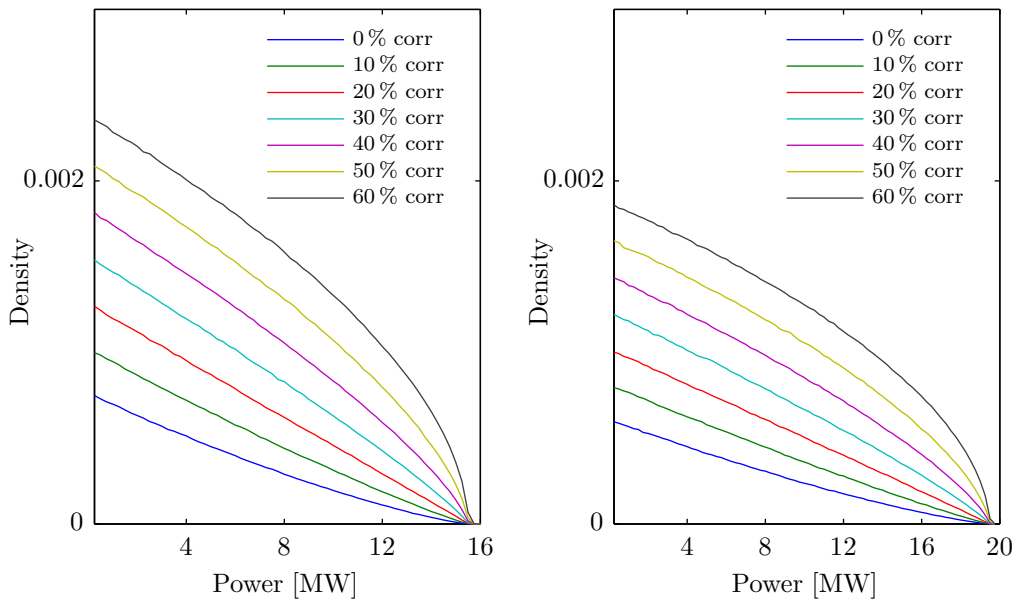


Figure 5.22: Simulation result for branch 2 with a line limit of 180 MW



(a) PDF of storage device St_1 at bus B

(b) PDF of storage device St_2 at bus C

Figure 5.23: Probability density functions of storages at injection buses

Chapter 6

Conclusion

Based on the method of generation positively correlated, β -distributed random variables from Magnussen [106], we modified the algorithm and added a compensation for the bias. We applied a set of random variables ranging from 0% to 100% correlation to our probabilistic load flow simulations as input and derived a set of corresponding PDFs of each line flow as output. As final part of our simulations we added transmission limits to lines and storage devices to the injection buses. We used the DC load flow method with PTDFs and the Monte Carlo simulation for our computations.

Our main focus was to find an algorithm for generating positively correlated, β -distributed random variables to reach the desired correlation levels as closely as possible. We adopted the method from Magnussen at first and added compensation in a second step to narrow our margin of error. With our developed method we are able to generate sets of β -distributed random variables with an exactly specified correlation.

The generation of β -distributed random variables with a specific correlation is tested for positive correlation and parameters where $\beta > \alpha$.

Depending on the correlation factors among all random variables the number of random variables generated is limited. The higher the correlation factors among the random variables, the lower the count of generated random variables. To find the possible correlation combinations among multiple random variables is a general mathematical problem. The best way to show the different combinations of correlation is by the means of a correlation matrix.

We used this method to generate our input variables and ran different simulations. We started our research by investigating the influence of two identical wind farms to the probability density functions of the lines for the entire range of correlation.

In this case, the original curve matches the 100% correlation curve. The same thing is true for the convolution result and the 0% curve. As one very

important result we found out that the curves of maximum and minimum correlation are the marginal curves of an area where all other curves are lying in. There is also a transformation from the maximal to the minimal curve with respect to the correlation.

We can specify the maximum and minimum loads of a line by just looking at the combination of these two curves of extremes. For the maximum and minimum values of line loads we only need to calculate the convolution of the input variables and combine it with the original distribution. No additional computations are required. Minor inaccuracies can only be found at the intersection points.

For a specific correlation level we are able to calculate the resulting line load by running the full computation. This result can be used to find the optimal value of line load for dimensioning the lines with respect to the economic transmission capacity. On the other hand, we can obtain the requirements of what a line must be able to handle.

We also looked at different wind farms and their impact on the line distributions. Different wind farms require other parameters for both of the β -distributions. The maximum correlation depends on the variety of the input distributions. The results are similar. The curve of the maximum correlation must be computed this time. The curves of the maximum and minimum are again the borders of the areas where all other correlation curves are lying in.

These two graphs illustrate again the extreme values of the line loads. Thus, a general statement of the load of the lines can be given by the graphs of their extremes.

To sum it all up, we can conclude, that our method can compute the probability density function of a line load for a certain correlation among β -distributed random variables. If no specific correlation is given, we can determine the range of the line load as an area bounded by the minimum and maximum of possible line loads.

The scalability of this method is restricted by the mathematical constraints of possible correlation factors among multiple random variables. If it is possible that many random variables are correlated to each other, every shared random variable is only a very small part of the whole β -distributed random variable and this can affect the accuracy of the reached correlation.

Finally, we added storage devices to the injection buses and introduced line limits. For the distribution of the line flow we found out that the density function of the limited line looks the same up to the limit and then it is zero. At the value of the limit there is a peak because every power flow event above the limit now occurs at the limit value.

The probability density function of the storage exactly matches the area

of the line distribution above the limit, which is cut. The power flow values of course are of the storage are the values above the limit minus the limit value. The power flow including this difference occurs on the line at the limit and results in the peak.

Unfortunately, this is the only result we can get out of the storage simulation by a probabilistic method. The main problem is that this method has no information about time and/or order as well as dependencies of the occurrences. This limits the applicability of our method for any considerations related to storage. Our result represents the density function of only filling the storage.

List of Figures

1.1	Global energy consumption	1
1.2	Global cumulatively installed wind	2
2.1	Basic 2 bus and 1 branch DC power flow model	8
3.1	Flow chart	22
3.2	Positive correlation, same shape	24
3.3	Positive correlation, contrary shape	25
3.4	Negative correlation, same shape	26
3.5	Negative correlation, contrary shape	27
3.6	Correlation characteristics	28
3.7	Compensated positive correlation, same shape	30
3.8	Correlation characteristics for different shapes	32
3.9	Intersection areas	34
3.10	Linear interpolation result	35
3.11	Simulation result with overlaid linear interpolation result	36
4.1	Effective DC load flow model with 3 buses and 3 branches	37
4.2	DC load flow model with 4 buses and 4 branches	38
4.3	Load profile	40
4.4	IEEE 14-bus test case	43
4.5	Load flow model with 4 buses, 4 branches and 2 storage devices	44
5.1	Identical PDF for wind power injections W_1 and W_2	45
5.2	Simulation result for branch 1 including flow direction	46
5.3	Simulation result for branch 2 including flow direction	47
5.4	Simulation result for branch 3 including flow direction	48
5.5	Simulation result for branch 1 with absolute values	48
5.6	Simulation result for branch 2 with absolute values	49
5.7	Simulation result for branch 3 with absolute values	49
5.8	Load flow minimum and maximum of branch 1	50
5.9	Load flow minimum and maximum of branch 2	50

5.10	Load flow minimum and maximum of branch 3	51
5.11	Different PDFs for wind power injections W_1 and W_2	52
5.12	Simulation result for branch 1 with flow direction	53
5.13	Simulation result for branch 2 with flow direction	54
5.14	Simulation result for branch 3 with flow direction	54
5.15	Simulation result for branch 1 with absolute values	55
5.16	Simulation result for branch 2 with absolute values	55
5.17	Simulation result for branch 3 with absolute values	56
5.18	Load flow minimum and maximum of branch 1	56
5.19	Load flow minimum and maximum of branch 2	57
5.20	Load flow minimum and maximum of branch 3	57
5.21	Simulation result for branch 1 with line limit	58
5.22	Simulation result for branch 2 with line limit	59
5.23	PDFs of storage devices at injection buses	59

List of Tables

3.1	Random variable correlation by different methods	31
4.1	Definition of line parameters for 3 bus and 3 branch test system	38
4.2	Definition of line parameters for 4 bus and 4 branch test system	39
4.3	Example correlation matrix with 3 buses	41
4.4	Example correlation matrix with 8 buses	42

List of Abbreviations

AC alternating current

CDF cumulative density function

corr correlation

DC direct current

IEEE Institute of Electrical and Electronics Engineers

MC Monte Carlo

NaN not a number

PDF probabilistic density function

PDTF power transfer distribution factor

PLF probabilistic load flow

PPF probabilistic power flow

RV random variable

SoC state of charge

Bibliography

- [1] OECD. *World Energy Outlook 2010*. OECD Publishing, 2010.
- [2] Global Wind Energy Council. Global Wind Report - Annual market update 2010. http://www.gwec.net/fileadmin/images/Publications/GWEC_annual_market_update_2010_-_2nd_edition_April_2011.pdf, April 2011.
- [3] Bonneville Power Administration. Homepage. <https://www.bpa.gov>, July 20, 2011.
- [4] ERCOT. Electric Reliability Council of Texas. Homepage. <http://www.ercot.com>, July 2010.
- [5] Midwest ISO. Midcontinent Independent System Operator. Homepage. <https://www.misoenergy.org>, July 2010.
- [6] National Renewable Energy Laboratory. Example of Wind Energy Curtailment Practices. <http://www.nrel.gov/docs/fy10osti/48737.pdf>, July 2010.
- [7] G. Brauner. *Vorlesungsunterlagen zu Energieversorgung*. Vienna University of Technology, Vienna, 2006.
- [8] Xi Lu, Michael B. McElroy, and Juha Kiviluoma. Global potential for wind-generated electricity. *Proceedings of the National Academy of Sciences*, 2009.
- [9] B. Borkowska. Probabilistic load flow. *Power Apparatus and Systems, IEEE Transactions on*, PAS-93(3):752–759, May 1974.
- [10] P. Chen, Z. Chen, and B. Bak-Jensen. Probabilistic load flow: A review. In *Electric Utility Deregulation and Restructuring and Power Technologies, 2008. DRPT 2008. Third International Conference on*, pages 1586–1591, April 2008.

-
- [11] H. Louie. Evaluation of probabilistic models of wind plant power output characteristics. In *Probabilistic Methods Applied to Power Systems (PMAPS), 2010 IEEE 11th International Conference on*, pages 442–447, June 2010.
- [12] H. Louie. Characterizing and modeling aggregate wind plant power output in large systems. In *Power and Energy Society General Meeting, 2010 IEEE*, pages 1–8, July 2010.
- [13] T.J. Overbye, Xu Cheng, and Yan Sun. A comparison of the ac and dc power flow models for lmp calculations. *Hawaii International Conference on System Sciences*, 2:1–9, January 2004.
- [14] G. Andersson. *Modelling and Analysis of Electric Power Systems*. Swiss Federal Institute of Technology Zurich, Zurich, September 2008. http://www.eeh.ee.ethz.ch/uploads/tx_ethstudies/modelling_hs08_script_02.pdf.
- [15] K. Purchala, L. Meeus, D. Van Dommelen, and R. Belmans. Usefulness of dc power flow for active power flow analysis. In *Power Engineering Society General Meeting, 2005. IEEE*, volume 1, pages 454–459, June 2005.
- [16] B. Stott, J. Jardim, and O. Alsac. Dc power flow revisited. *Power Systems, IEEE Transactions on*, 24(3):1290–1300, August 2009.
- [17] C. Barbulescu, S. Kilyeni, G. Vuc, B. Lustrea, R.-E. Precup, and S. Preid. Software tool for power transfer distribution factors (ptdf) computing within the power systems. In *EUROCON 2009, EUROCON '09. IEEE*, pages 517–524, May 2009.
- [18] Kang Chang and Xueshan Han. Study on dominant path of power grid under a given operation mode part ii: Proof in dc power flow systems. In *Power Engineering Conference, 2007. IPEC 2007. International*, pages 872–876, December 2007.
- [19] A.G. Bakirtzis and P.N. Biskas. Decentralised dc load flow and applications to transmission management. *Generation, Transmission and Distribution, IEE Proceedings-*, 149(5):600–606, September 2002.
- [20] C.Y. Evrenosoglu and A. Abur. Effects of measurement and parameter uncertainties on the power transfer distribution factors. In *Probabilistic Methods Applied to Power Systems, 2004 International Conference on*, pages 608–611, September 2004.

-
- [21] Xu Cheng and T.J. Overbye. Ptdf-based power system equivalents. *Power Systems, IEEE Transactions on*, 20(4):1868–1876, November 2005.
- [22] Minghai Liu and G. Gross. Role of distribution factors in congestion revenue rights applications. *Power Systems, IEEE Transactions on*, 19(2):802–810, May 2004.
- [23] Kaigui Xie, Chunyan Li, and Yenren Liu. Tracing power flow from generators to loads and branches using incidence matrix multiplication. In *Power Energy Society General Meeting, 2009. PES '09. IEEE*, pages 1–7, July 2009.
- [24] R. Baldick. Variation of distribution factors with loading. *Power Systems, IEEE Transactions on*, 18(4):1316–1323, November 2003.
- [25] M. Zhao, Z. Chen, and F. Blaabjorg. Probabilistic capacity of a grid connected wind farm. In *Industrial Electronics Society, 2005. IECON 2005. 31st Annual Conference of IEEE*, pages 774–779, November 2005.
- [26] Liang Min and Pei Zhang. A probabilistic load flow with consideration of network topology uncertainties. In *Intelligent Systems Applications to Power Systems, 2007. ISAP 2007. International Conference on*, pages 1–5, November 2007.
- [27] M.A. Laughton and M.W. Humphrey Davies. Numerical techniques in solution of power-system load-flow problems. *Electrical Engineers, Proceedings of the Institution of*, 111(9):1575–1588, September 1964.
- [28] B. Stott. Review of load-flow calculation methods. *Proceedings of the IEEE*, 62(7):916–929, July 1974.
- [29] J. Biricz and H. Müller. Probabilistische Lastflußberechnung. *Electrical Engineering (Archiv für Elektrotechnik)*, 64:77–84, 1981.
- [30] P. Chen, Z. Chen, and B. Bak-Jensen. Probabilistic load flow: A review. In *Electric Utility Deregulation and Restructuring and Power Technologies, 2008. DRPT 2008. Third International Conference on*, pages 1586–1591, april 2008.
- [31] J.F. Dopazo, O.A. Klitin, and A.M. Sasson. Stochastic load flows. *Power Apparatus and Systems, IEEE Transactions on*, 94(2):299–309, March 1975.

- [32] J. Vorsic, V. Muzek, and G. Skerbinek. Stochastic load flow analysis. In *Electrotechnical Conference, 1991. Proceedings., 6th Mediterranean*, volume 2, pages 1445–1448, May 1991.
- [33] M.S. Kang, C.S. Chen, Y.L. Ke, and T.E. Lee. Stochastic load flow analysis by considering temperature sensitivity of customer power consumption. In *Power Tech Conference Proceedings, 2003 IEEE Bologna*, volume 3, page 6 pp., June 2003.
- [34] Dongtao Wang and Yixin Yu. Probabilistic static voltage stability security assessment for power transmission system. In *Power and Energy Engineering Conference (APPEEC), 2010 Asia-Pacific*, pages 1–4, March 2010.
- [35] H.R. Sirisena and E.P.M. Brown. Representation of non-gaussian probability distributions in stochastic load-flow studies by the method of gaussian sum approximations. *Generation, Transmission and Distribution, IEE Proceedings C*, 130(4):165–71, July 1983.
- [36] R.N. Allan, B. Borkowska, and C.H. Grigg. Probabilistic analysis of power flows. *Electrical Engineers, Proceedings of the Institution of*, 121(12):1551–1556, December 1974.
- [37] R.N. Allan and M.R.G. Al-Shakarchi. Probabilistic a.c. load flow. *Electrical Engineers, Proceedings of the Institution of*, 123(6):531–536, June 1976.
- [38] R.N. Allan, C.H. Grigg, D.A. Newey, and R.F. Simmons. Probabilistic power-flow techniques extended and applied to operational decision making. *Electrical Engineers, Proceedings of the Institution of*, 123(12):1317–1324, December 1976.
- [39] R. N. Allan, C. H. Grigg, and M. R. G. Al-Shakarchi. Numerical techniques in probabilistic load flow problems. *International Journal for Numerical Methods in Engineering*, 10(4):853–860, 1976.
- [40] R.N. Allan and M.R.G Al-Shakarchi. Probabilistic techniques in a.c. load-flow analysis. *Electrical Engineers, Proceedings of the Institution of*, 124(2):154–160, February 1977.
- [41] R.N. Allan and M.R.G. Al-Shakarchi. Linear dependence between nodal powers in probabilistic a.c. load flow. *Electrical Engineers, Proceedings of the Institution of*, 124(6):529–534, June 1977.

- [42] R.N. Allan, A.M. Leite da Silva, and R.C. Burchett. Evaluation methods and accuracy in probabilistic load flow solutions. *Power Apparatus and Systems, IEEE Transactions on*, PAS-100(5):2539–2546, May 1981.
- [43] R.N. Allan, A.M. Leite da Silva, A.A. Abu-Nasser, and R.C. Burchett. Discrete convolution in power system reliability. *Reliability, IEEE Transactions on*, R-30(5):452–456, December 1981.
- [44] A.M. Leite da Silva, V.L. Arienti, and R.N. Allan. Probabilistic load flow considering dependence between input nodal powers. *Power Apparatus and Systems, IEEE Transactions on*, PAS-103(6):1524–1530, June 1984.
- [45] A. Dimitrovski and R. Ackovski. Probabilistic load flow in radial distribution networks. In *Transmission and Distribution Conference, 1996. Proceedings., 1996 IEEE*, pages 102–107, September 1996.
- [46] S. Beharrysingh and C. Sharma. Development and application of a probabilistic simulation program for long term system planning. In *Probabilistic Methods Applied to Power Systems, 2006. PMAPS 2006. International Conference on*, pages 1–9, June 2006.
- [47] J. Schwippe, O. Krause, and C. Rehtanz. Extension of a probabilistic load flow calculation based on an enhanced convolution technique. In *Sustainable Alternative Energy (SAE), 2009 IEEE PES/IAS Conference on*, pages 1–6, September 2009.
- [48] F. Coroiu, D. Dondera, C. Velicescu, and G. Vuc. Power systems reliability evaluation using probabilistic load flows methods. In *Universities Power Engineering Conference (UPEC), 2010 45th International*, pages 1–5, 31st August - 3rd September 2010.
- [49] D. Villanueva, J.L. Pazos, and A. Feijóo. Probabilistic load flow including wind power generation. *Power Systems, IEEE Transactions on*, 26(3):1659–1667, August 2011.
- [50] A. Papoulis and S.U. Pillai. *Probability, random variables, and stochastic processes*. McGraw-Hill electrical and electronic engineering series. McGraw-Hill, fourth edition, 2002.
- [51] P.A. Bromiley. Products and convolutions of gaussian distributions. Internal Report 2003-003, TINA Vision, 2003.

- [52] B.W. Lindgren. *Statistical Theory*. Texts in Statistical Science Series. Chapman & Hall, 1993.
- [53] R. A. Fisher. Moments and product moments of sampling distributions. *Proceedings of the London Mathematical Society*, s2-30(1):199–238, 1930.
- [54] M.G. Kendall and A. Stuart. *The Advanced Theory of Statistics: Distribution theory*. The Advanced Theory of Statistics. Macmillan, 1977.
- [55] A. Hald. The early history of the cumulants and the gram-charlier series. *International Statistical Review / Revue Internationale de Statistique*, 68(2):137–153, 2000.
- [56] H.H. Crapo, D. Senato, and G.C. Rota. *Algebraic Combinatorics and Computer Science: A Tribute to Gian-Carlo Rota*. Springer, 2001.
- [57] Li Xiaoming, Chen Xiaohui, Yin Xianggen, Xiang Tiejuan, and Liu Huagang. The algorithm of probabilistic load flow retaining nonlinearity. In *Power System Technology, 2002. Proceedings. PowerCon 2002. International Conference on*, volume 4, pages 2111–2115, 2002.
- [58] R. Von Mises. *Mathematical theory of probability and statistics*. Academic Press, New York, 1964.
- [59] Z. Hu and Xifan Wang. A probabilistic load flow method considering branch outages. *Power Systems, IEEE Transactions on*, 21(2):507–514, May 2006.
- [60] L.A. Sanabria and T.S. Dillon. Stochastic power flow using cumulants and von mises functions. *International Journal of Electrical Power and Energy Systems*, 8(1):47–60, 1986.
- [61] J.E. Kolassa. *Series Approximation Methods in Statistics*, volume 88 of *Lecture Notes in Statistics*. Springer New York, third edition, 2006.
- [62] S. Patra and R.B. Misra. Probabilistic load flow solution using method of moments. In *Advances in Power System Control, Operation and Management, 1993. APSCOM-93., 2nd International Conference on*, volume 2, pages 922–934, December 1993.
- [63] Pei Zhang and S.T. Lee. A new computation method for probabilistic load flow study. In *Power System Technology, 2002. Proceedings. PowerCon 2002. International Conference on*, volume 4, pages 2038–2042, October 2002.

- [64] Pei Zhang and S.T. Lee. Probabilistic load flow computation using the method of combined cumulants and gram-charlier expansion. *Power Systems, IEEE Transactions on*, 19(1):676–682, February 2004.
- [65] A. Schellenberg, W. Rosehart, and J. Aguado. Cumulant-based probabilistic optimal power flow (p-opf) with gaussian and gamma distributions. *Power Systems, IEEE Transactions on*, 20(2):773–781, May 2005.
- [66] A. Tamtum, A. Schellenberg, and W.D. Rosehart. Enhancements to the cumulant method for probabilistic optimal power flow studies. *Power Systems, IEEE Transactions on*, 24(4):1739–1746, November 2009.
- [67] Dong Lei, Zhang Chuan-cheng, Yang Yi-han, and Zhang Pei. Improvement of probabilistic load flow to consider network configuration uncertainties. In *Power and Energy Engineering Conference, 2009. APPEEC 2009. Asia-Pacific*, pages 1–5, March 2009.
- [68] Miao Lu, Zhao Yang Dong, and T.K. Saha. A probabilistic load flow method considering transmission network contingency. In *Power Engineering Society General Meeting, 2007. IEEE*, pages 1–6, June 2007.
- [69] Jian Ma, Zhenyu Huang, Pak Chung Wong, Tom Ferryman, and Pacific Northwest. Probabilistic vulnerability assessment based on power flow and voltage distribution. In *Transmission and Distribution Conference and Exposition, 2010 IEEE PES*, pages 1–8, April 2010.
- [70] Ying-Yi Hong and Yi-Feng Luo. Optimal var control considering wind farms using probabilistic load-flow and gray-based genetic algorithms. *Power Delivery, IEEE Transactions on*, 24(3):1441–1449, July 2009.
- [71] Lei Dong, Saifeng Li, Yihan Yang, and Hai Bao. The calculation of transfer reliability margin based on the probabilistic load flow. In *Power and Energy Engineering Conference (APPEEC), 2010 Asia-Pacific*, pages 1–4, March 2010.
- [72] J.W. Stahllhut, G.T. Heydt, and G.B. Sheble. A stochastic evaluation of available transfer capability. In *Power Engineering Society General Meeting, 2005. IEEE*, volume 3, pages 3055–3061, June 2005.
- [73] Chun-Lien Su. A new probabilistic load flow method. In *Power Engineering Society General Meeting, 2005. IEEE*, volume 1, pages 389–394, June 2005.

- [74] E. Rosenblueth. Point estimation for probability moments. *Proceedings of the National Academy of Sciences USA*, 72(10):3812–3814, 1975.
- [75] E. Rosenblueth. Two point estimates in probabilities. *Applied Mathematical Modelling*, 5(5):329–335, 1982.
- [76] J.M. Morales and J. Perez-Ruiz. Point estimate schemes to solve the probabilistic power flow. *Power Systems, IEEE Transactions on*, 22(4):1594–1601, November 2007.
- [77] G. Verbic and C.A. Canizares. Probabilistic optimal power flow in electricity markets based on a two-point estimate method. *Power Systems, IEEE Transactions on*, 21(4):1883–1893, November 2006.
- [78] G. Mokhtari, A. Rahiminezhad, A. Behnood, J. Ebrahimi, and G.B. Gharehpetian. Probabilistic dc load-flow based on two-point estimation (t-pe) method. In *Power Engineering and Optimization Conference (PEOCO), 2010 4th International*, pages 1–5, June 2010.
- [79] J.M. Morales, L. Baringo, A.J. Conejo, and R. Minguez. Probabilistic power flow with correlated wind sources. *Generation, Transmission Distribution, IET*, 4(5):641–651, May 2010.
- [80] S.R. Jaschke. The cornish-fisher-expansion in the context of delta - gamma - normal approximations. Sonderforschungsbereich 373 2001-54, version 1.41, Humboldt Universität Berlin, December 4, 2001.
- [81] Shujun Yao, Yan Wang, Minxiao Hang, and Xiaona Liu. Research on probabilistic power flow of the distribution system with wind energy system. In *Critical Infrastructure (CRIS), 2010 5th International Conference on*, pages 1–6, September 2010.
- [82] Shujun Yao, Yan Wang, Minxiao Hang, and Xiaona Liu. Research on probabilistic power flow of the distribution system with photovoltaic system generation. In *Power System Technology (POWERCON), 2010 International Conference on*, pages 1–6, October 2010.
- [83] Tang Gui-kun, Yao Shu-jun, and Wang Yan. Research on probabilistic power flow of the distribution system based on cornish-fisher. In *Power and Energy Engineering Conference (APPEEC), 2011 Asia-Pacific*, pages 1–5, March 2011.
- [84] J. Usaola. Probabilistic load flow with wind production uncertainty using cumulants and cornish-fisher expansion. *International Journal of Electrical Power and Energy Systems*, 31(9):474–481, 2009.

- [85] J. Usaola. Probabilistic load flow in systems with wind generation. *Generation, Transmission Distribution, IET*, 3(12):1031–1041, December 2009.
- [86] Julio Usaola. Probabilistic load flow with correlated wind power injections. *Electric Power Systems Research*, 80(5):528–536, 2010.
- [87] V. Miranda and J.P. Saraiva. Fuzzy modelling of power system optimal load flow. *Power Systems, IEEE Transactions on*, 7(2):843–849, May 1992.
- [88] P. Gajalakshmi and S. Rajesh. Fuzzy modeling of power flow solution. In *Telecommunications Energy Conference, 2007. INTELEC 2007. 29th International*, pages 923–927, September 30–October 4 2007.
- [89] M.A. Matos and E.M. Gouveia. The fuzzy power flow revisited. *Power Systems, IEEE Transactions on*, 23(1):213–218, February 2008.
- [90] C.P. Robert and G. Casella. *Monte Carlo Statistical Methods*. Springer Texts in Statistics. Springer, 2004.
- [91] R.N. Allan and A.M. Leite da Silva. Probabilistic load flow using multilinearisations. *Generation, Transmission and Distribution, IEE Proceedings C*, 128(5):280–287, September 1981.
- [92] A.M. Leite da Silva and V.L. Arienti. Probabilistic load flow by a multilinear simulation algorithm. *Generation, Transmission and Distribution, IEE Proceedings C*, 137(4):276–282, July 1990.
- [93] H. Mori and Wenjun Jiang. A new probabilistic load flow method using mcmc in consideration of nodal load correlation. In *Intelligent System Applications to Power Systems, 2009. ISAP '09. 15th International Conference on*, pages 1–6, November 2009.
- [94] C. Barbulescu, Gh. Vuc, S. Kilyeni, D. Jigoria-Oprea, and O. Pop. Transmission planning - a probabilistic load flow perspective. *Proceedings of World Academy of Science, Engineering and Technology*, pages 666–671, August 2008.
- [95] C. Barbulescu, G. Vuc, and S. Kilyeni. Probabilistic power flow approach for complex power system analysis. In *Human System Interactions, 2008 Conference on*, pages 551–556, May 2008.

- [96] L.B. Shi, C. Wang, L.Z. Yao, L.M. Wang, Y.X. Ni, and B. Masoud. Optimal power flow with consideration of wind generation cost. In *Power System Technology (POWERCON), 2010 International Conference on*, pages 1–5, October 2010.
- [97] D. Villanueva, A. Feijóo, and J. Pazos. Probabilistic load flow considering correlation between generation, loads and wind power. *Smart Grid and Renewable Energy*, 2(1):12–20, 2011.
- [98] D.J. Burke and M.J. O’Malley. Optimal wind power location on transmission systems - a probabilistic load flow approach. In *Probabilistic Methods Applied to Power Systems, 2008. PMAPS ’08. Proceedings of the 10th International Conference on*, pages 1–8, May 2008.
- [99] N.L. Johnson, S. Kotz, and N. Balakrishnan. *Continuous Univariate Distributions*, volume 1 of *Wiley series in probability and mathematical statistics. Probability and mathematical statistics*. Wiley & Sons, New York, second edition, 1994.
- [100] N.L. Johnson, S. Kotz, and N. Balakrishnan. *Continuous Univariate Distributions*, volume 2 of *Wiley series in probability and mathematical statistics. Probability and mathematical statistics*. Wiley & Sons, New York, second edition, 1995.
- [101] Roger B. Nelsen. *An Introduction to Copulas*. Springer Texts in Statistics. Springer New York, 2006.
- [102] V. Dukic and N. Maric. On construction of random variables with prescribed marginal distributions and correlation coefficients. *arXiv:1010.6118v1 [math.PR]*, pages 1–15, October 29, 2010.
- [103] K. Gross, J.R. Lockwood, C.C. Frost, and W.F. Morris. Modeling controlled burning and trampling reduction for conservation of hudsonia montana. *Conservation Biology*, 12(6):1291–1301, December 1998.
- [104] C.T. Dos Santos Dias, A. Samaranayaka, and B. Manly. On the use of correlated beta random variables with animal population modelling. *Ecological Modelling*, 215(4):293–300, 2008.
- [105] M. Catalani. Sampling from a couple of positively correlated beta variates. *ArXiv:math/0209090v1 [math.PR]*, pages 1–7, September 9, 2002.

- [106] Steen Magnussen. An algorithm for generating positively correlated beta-distributed random variables with known marginal distributions and a specified correlation. *Computational Statistics & Data Analysis*, 46(2):397–406, 2004.
- [107] Bonneville Power Administration. BPA Balancing Authority Load & Total Wind Generation. <http://transmission.bpa.gov/Business/Operations/Wind/default.aspx>, July 20, 2011.
- [108] W. Group. Common Format For Exchange of Solved Load Flow Data. *Power Apparatus and Systems, IEEE Transactions on*, PAS-92(6):1916–1925, 1973.
- [109] University of Washington. Power Systems Test Case Archive - IEEE Common Data Format. <http://www.ee.washington.edu/research/pstca/formats/cdf.txt>, July 20, 2011.
- [110] University of Washington. Power Systems Test Case Archive - 14 Bus Power Flow Test Case. http://www.ee.washington.edu/research/pstca/pf14/pg_tca14bus.htm, July 20, 2011.